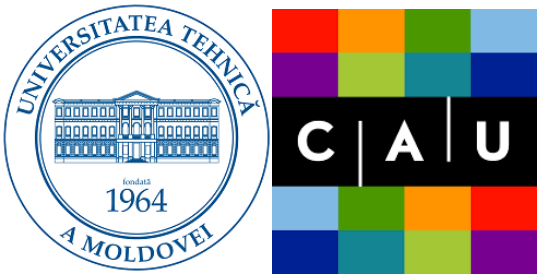

TECHNICAL UNIVERSITY OF MOLDOVA

AND KIEL UNIVERSITY

As a manuscript

UDC: 539.2:620.3:681.586(043.2)

RAJAT

POROUS NETWORKS OF NANOSTRUCTURED HYBRID MATERIALS

134.03 PHYSICS OF NANOSYSTEMS AND NANOTECHNOLOGIES

Summary of the doctoral thesis in Physical Sciences (Technical University of Moldova) and Engineering (Kiel University) (Joint degree)

Conducători Științifici:
LUPAN Oleg, Habilitated Doctor, University Professor, Technical University of Moldova
ADELUNG Rainer, Doctor rer. nat., University Professor, Kiel University (CAU), Germany

CHIȘINĂU, KIEL, 2026

The Ph.D. thesis was carried out within the Department of **Microelectronics and Biomedical Engineering,** Center of Nanotechnology and Nanosensors at the **Technical University of Moldova (UTM)** and the Department of **Materials Science, Kiel University.**
The Doctoral School of the Technical University of Moldova

Author: RAJAT
Scientific supervisors:

LUPAN Oleg	Habilitated Doctor in Engineering, University Professor, Technical University of Moldova
ADELUNG Rainer	Doctor rer. nat., University Professor, Kiel University (CAU), Germany

Committee for public defense (CSP):
TRONCIU Vasile, Habilitated Doctor in Physical and Mathematical Sciences, University Professor, Technical University of Moldova, Vice-Rector for research, President CSP
LUPAN Oleg, Habilitated Doctor of Engineering, University Professor, Technical University of Moldova, Scientific supervisor at UTM
ADELUNG Rainer, Doctor rer. nat., University Professor, Kiel University (CAU), Scientific supervisor at CAU
BUZDUGAN Artur, Habilitated Doctor in Physical Sciences, University Professor, Technical University of Moldova, Official reviewer
WULFINGHOFF Stephan, Doctor -Eng., University Professor, Kiel University (CAU), Germany, Official reviewer
SPRINCEAN Veaceslav, Doctor of Physical Sciences, Associate Professor, State University of Moldova, Official reviewer

The defense will take place on 09 April 2026, at 14:00 in the meeting of the Doctoral Commission within the Doctoral School of the Technical University of Moldova (approved by the decision of the Scientific Council of UTM on 27.02.2026, protocol no. 3), 9/7 Studentilor street, Building 3, Room 3-405, MD-2068, Chisinau, Republic of Moldova.

The doctoral thesis and the abstract are available for consultation at the library of the Technical University of Moldova and on the ANACEC website (https.//www.anacec.md/).

The summary was sent on **06 March 2026**

Author _____ Rajat

Scientific supervisor
Habilitated Doctor of Engineering, Professor _____ LUPAN Oleg

Doctor rer. nat., Professor _____ ADELUNG Rainer

RESEARCH CONCEPT GUIDELINES

Description of the topic:

Metal-organic frameworks (MOFs) are among the most promising materials in the development of porous structures and gas sensors due to their modular nature which facilitates the incorporation of specific functional groups for the customization of the structure of MOFs and the presence of flexible cavities which allows molecules of specific size to pass through due to the molecular sieving effect [1,2]. As the Nobel Prize foundation highlighted in 2025, designing and synthesis of materials at the molecular level (such as MOFs) is essential for addressing global challenges, from extracting CO_2 to extracting drinking water from desert air [3]. A continuous decline in the environmental quality can be observed due to a combination of human activities, wars and natural factors. To tackle this issue, researchers have been developing novel materials and studying their properties to employ them in the field of gas sensing and the development of porous frameworks for cabon dioxide capture. Continuous monitoring using MOFs is necessary to control and limit emissions of volatile organic compound (VOC). Real-time monitoring of VOCs-exposure to each individual, spatial environmental monitoring and scientific research can help mitigate their harmful effects. However, in the ambient environment, the simultaneous presence of 50-300 VOCs [4], as well as extreme humidity variations, and temperature variations make accurate detection of target gas very challenging. Bare metal oxide-based gas sensors have limitations such as high operating temperature, poor selectivity, etc. The development of hybrid materials can improve the issue of selectivity and endurance against humidity. MOFs are porous framework materials that possess properties such as ultra-high specific surface area, preferential interaction sites, and structural flexibility. When used as an additional layer, they can act as concentrators, providing selective diffusion pathways that facilitate the transport of specific analytes to the sensing interface. Furthermore, with advances in technology and data analytics, different VOCs can be differentiated through the simultaneous or sequential detection of responses from individual sensors in sensor arrays. Thus, the synergistic effect of metal oxides and MOFs or other functionalized materials synthesized and deposited by the different techniques contribute to the development of more sensitive and selective materials, with high stability even under adverse environmental conditions.

The importance of the addressed problem:

The advancements in material design by employing hybrids combining metal oxides and zeolitic imidazolate frameworks (ZIFs), a special class of MOFs, for their synergistic effect has revolutionized modern materials science. The synergistic interaction between the metal oxide and MOF components in hybrid structures significantly enhances sensing performance by integrating the complementary properties of each component and mitigating the limitations associated with bare metal oxide-based sensors. The development of robust hybrid structures based on metal-organic frameworks-metal oxide systems is of great significance in the field of gas sensing [1,5–7]. Numerous gas-sensing materials have been employed in the field of gas sensing, including ZnO, CuO, mixed oxides such as tetrapodal ZnO (t-ZnO) and CuO nanostructures, etc [8,9]. The primary limitations of metal-oxide-based gas sensors are non-withstanding against humidity, poor selectivity, and signal drift, etc [9]. An additional coating layer of hydrophobic MOFs on top of metal oxides can solve these issues of selectivity, stability, and humidity immunity by providing preferential interaction sites for the target analyte, utilizing the molecular sieving effect, or through

the doping or functionalization of an appropriate material. The hydrophobic properties, as the name suggests keep the sample stable even in high humidity conditions. There are lot of other factors that influence the sensing properties such as the morphology, porosity, specific surface area, and particle size of the sensing material. The doping concentration influences both the optical and the electrical properties of the sensing material by altering the charge carrier concentration, modifying absorption efficiency, and by introducing new energy levels within the band structure. Partial surface conversion of metal oxides creates additional active sites at the interface for interaction with target analytes, thereby enhancing sensing performance. For example, complete coverage of CuO nanoplatelets on a single t-ZnO microrod provides preferential interaction sites for hydrogen molecules, while the branched arms of the t-ZnO microrods hinder the diffusion of large VOC molecules, limiting their interaction at the interface [9].

Sequential detection of target analytes using a sensor array enables the differentiation of multiple gases (multicomponent detection) by analysing various output parameters, such as the sensing response, response time, recovery time, and optimum operating temperature. By incorporating diverse tools such as principal component analysis (PCA), the classification of analytes into distinct groups becomes more reliable based on differences in their principal component scores.

The goal and objectives of the research:

The doctoral thesis aims to: (i) synthesize advanced hybrid materials based on metal-organic frameworks (MOF/ZIF) and nanostructured metal oxides (MOx), specifically MOF/MOX architectures; (ii) develop and optimize high-performance hybrid sensors based on ZIF-71/CuO:Al, ZIF-8/CuO:Al, ZIF-67/ZnO, ZIF-7/ZnO, ZIF-71/ZnO, and ZIF-8/ZnO structures capable of ensuring selective and stable detection of hydrogen and volatile organic compounds (VOCs) under variable environmental conditions; and (iii) elucidate the physicochemical mechanisms governing gas-surface interactions to establish a predictive framework for the detection and discrimination of these analytes.

Proposed research objectives:

- Development of hybrid structures based on combinations of ZIF (ZIF-67, -7, -71, -8) and metal oxides (CuO:Al, ZnO:Cd) using a simple and cost-effective approaches, such as synthesis from chemical solutions (SCS) for oxides and room-temperature drop-casting of MOFs for the assembly of sensing structures.
- Advanced evaluation of the physicochemical properties of ZIF-8/CuO:Al hybrid structures and correlate them with sensing performance (sensitivity and selectivity) towards hydrogen and n-butanol (among VOCs), under adverse environmental conditions over an extended period.
- Comprehensive investigation of the physicochemical properties of ZIF-71/CuO:Al structures and establishment of structure-property-sensing performance correlations toward hydrogen and n-butanol at different operating temperatures over an extended period.
- Achieving selective detection and discrimination of various analytes (VOCs and hydrogen gas) with distinct sensitivity profiles, achieved through sequential detection using ZIF-67/ZnO, ZIF-7/ZnO, ZIF-8/ZnO și ZIF-71/ZnO-based sensor platforms.
- Elucidation of gas-surface interaction mechanisms was proposed by integrating ionosorption model, transport physics, and electronic-structure parameters (polarizability and

dipole moments) to establish a predictive framework for the selective recognition of analytes using ZIF/metal-oxide hybrid structures.

Scientific research methodology:

To achieve the objectives of this work, the following technological and scientific research methods were employed:

- ZnO, CuO, Cd-doped ZnO, and Al-doped CuO were synthesized using a SCS approach, followed by heat treatment via conventional thermal annealing or rapid thermal annealing in air.
- ZIFs were synthesized at room temperature, and dispersions of ZIF particles were prepared in methanol/2-propanol. Subsequently, hybrid metal-organic framework/metal oxide (MOF/MO) structures, namely ZIF/ZnO- or ZIF/CuO-based hybrid structures were fabricated using a simple and cost-effective SCS technique followed by drop-casting.
- The morphology, grain size, and distribution of the synthesized metal oxides, as well as the distribution of ZIFs on the metal oxide surfaces, were investigated using scanning electron microscopy (SEM).
- The structural properties, phase transitions, phase transformations, and crystallinity of the developed hybrid materials were analyzed using X-ray diffraction (XRD) or temperature-dependent *in-situ* X-ray diffraction.
- Phonon modes associated with the different components of the hybrid materials were investigated using micro-Raman spectroscopy to elucidate their vibrational characteristics and structural interactions.
- Energy dispersive X-ray (EDX) and X-ray photoelectron spectroscopy (XPS) were used to determine the chemical composition, oxidation states, and bonding interactions of the different components of the developed MOF/MO hybrid material.
- The Keithley 2400 SourceMeter unit, controlled via a programable LabVIEW interface (National Instruments), was used to precisely characterize the electrical properties of the devices using a two-point probe configuration under different chemical environments for the evaluation of their sensing performance.
- Sensor characterization was performed using a custom-built apparatus integrated with a computer-controlled source meter (Keithley 2400 and 2450, Keithley, OH, USA). The gas-sensing performance was evaluated across various operating temperatures (OPTs). During the testing cycle, diverse analytes including hydrogen, n-butanol, 2-propanol, ethanol, acetone, ammonia, carbon dioxide, and methane were introduced into the test chamber at a fixed concentration of 100 ppm and different relative humidities.

Novelty of the obtained scientific results:

This work presents the development of hybrid materials based on nanostructured and microstructured metal-organic framework-metal oxide systems (MOF/MO), especially ZIF/ZnO and ZIF/CuO, were developed using a simple and cost-effective approach. The innovative contribution to the scientific community consists in the detailed investigation of the physicochemical properties of these hybrids and in the establishment of a rigorous methodology for correlating the structure-property-performance relationship for the selective detection of hydrogen and VOCs under adverse environmental conditions. (i) ZIF-8/CuO:Al-based hybrid structures are selective for hydrogen (>4 times) over other tested analytes (acetone, 2-propanol, n-butanol, and ethanol) at 350 °C. ZIF-8/CuO:Al-based hybrid structures exhibited an appreciable

response (75%) to 100 ppm hydrogen even at a high relative humidity of 81%, enabling their application under adverse humid conditions even for long periods of time. The developed hybrid structures demonstrated temporal stability and retains notable sensing performance for a long period of time, even after four weeks from the initial measurements. Furthermore, a very low detection limit of 402 ppb was achieved. (ii) ZIF-71/CuO:Al-based hybrid structures exhibited selectivity towards n-butanol at 200 ℃, with the sensing response being approximately four times higher than the response to hydrogen gas and approximately five times higher than the response to acetone during the initial measurements. The developed hybrid sensor exhibited dual gas sensing (n-butanol and hydrogen) at different operating temperatures (200 ℃ and 250 ℃, respectively), which can be attributed to the synergistic effect of ZIF-71 and CuO:Al. (iii) Temperature dependent *in-situ* XRD invesigation on four different ZIFs, including ZIF-n (n=67, 7, 71, and 8), provided detailed insights about the phase transitions, thermal degradation, and the transformation of ZIFs into their corresponding metal oxides (ZnO or Co_3O_4) at specific temperatures. The implementation of sequential gas detection of four studied ZIFs/ZnO hybrids and its Cd-doped ZnO counterparts demonstrated selectivity and optimal responses to 2-propanol, ethanol, n-butanol, and hydrogen under different operating conditions.

The scientific research problem solved:

The problem addressed in this work is to overcome the limitations of classical metal oxide-based sensors by developing advanced metal-organic framework/metal oxide (MOF/MO) hybrid materials. The synthesized hybrid materials-based on MOF/MO systems, including microstructures, nanostructures of metal oxides and ZIF-based hybrid structures, detect hydrogen, n-butanol, and 2-propanol under adverse environmental conditions. A fundamental understanding of the thermal degradation and phase transition mechanisms of the investigated ZIF-based MOFs was achieved by determining their thermal stability ranges, confirming stable operations of ZIF-67, ZIF-7, ZIF-71, and ZIF-8 structures. The ZIF-8/CuO:Al and ZIF-71/CuO:Al hybrid structure exhibited selectivity towards hydrogen gas even in the presence of extreme humidity conditions (RH 81%), with long-term temporal stability and detection of n-butanol and hydrogen at different operating temperatures. By combining *in-situ* analysis with sequential multi-sensor detection, the work established rigorous structure-property-performance correlations, enabling differentiation of analytes based on their distinct response signatures.

The theoretical significance:

The theoretical significance lies in establishing structure-property-performance relationships by determining the thermal stability ranges and oxidative transformation pathways of developed hybrid materials. These systems, based on ZIF-type metal-organic frameworks (ZIF-n (n=67, 7, 71, and 8)) and metal oxides through *in-situ* structural analysis, thus defining their fundamental operational limits and mechanistic contributions in gas sensing. Similarly, this work brings a critical understanding of the radiolytic stability of halogenated MOFs by identifying X-ray-induced degradation in ZIF-71, thus elucidating how specific functional groups dictate structural integrity under ionizing radiation and defining the thresholds necessary for non-destructive characterization. Furthermore, physicochemical models were developed to explain the gas-sensing mechanisms, incorporating concepts such as adsorption/desorption, activation energy, modulation of the potential barrier at the heterojunction interface, analyte's electronic polarizability, dipole moment of analyte, transport physics, and molecular sieving effect through ZIF pores, for VOCs and hydrogen at the interface of the ZIF/CuO:Al hybrid structures. Consequently, these findings

provide an underlying physical understanding of charge transport and molecular interactions at the hybrid interface, establishing a predictive framework for the optimization of selectivity in high-performance sensor technology. The work elucidates the role of charge transfer at the interface of heterostructures formed between metal oxides and ZIF phases, demonstrating how the modulation of the potential barrier and the depletion region contribute decisively to the sensor signal in the presence of target analytes.

The applicative values of the thesis consist of the following:

- The comparative analysis of thermal stability provided a fundamental roadmap for the thermal degradation of ZIFs within MOF/MOx systems, offering essential data for their integration into gas sensing devices. The research confirms the reliability of the materials by establishing safe operational limits: 250 °C (ZIF-67), 375 °C (ZIF-7), 350 °C (ZIF-71 and ZIF-8).
- The development of hybrid structures based on ZIF-8/CuO:Al, which demonstrated selective hydrogen gas detection with an extremely low limit of detection of approximately 402 ppb. This performance is essential for critical applications, such as detecting very small hydrogen leaks in energy infrastructures.
- The implementation of dual detection capability using ZIF-71/CuO:Al-based hybrid structures, which allow for the selective monitoring of n-butanol and hydrogen by modulating the operating temperature (200 °C and 250 °C, respectively). At 200 °C, the sensor exhibits a response to n-butanol four times higher than that for hydrogen gas, ensuring efficient discrimination of these analytes.
- The demonstration of the specific selectivity of the ZIF-67/ZnO hybrid sensor toward ethanol at 250 °C, whereas selectivity to hydrogen was observed for the other three hybrid structures: ZIF-7/ZnO, ZIF-71/ZnO, and ZIF-8/ZnO.
- The development and scalable fabrication of MOx and MOF/MOx systems based on synthesis from chemical solutions (SCS) and microdrop-casting techniques at room temperature, which requires low energy consumption and production cost compared to conventional methods, facilitating the integration of hybrid sensors into wearable devices.

Scientific thesis submitted for defense:

- Determination of the structural robustness, localization of defect states, and chemical configuration of metal organic frameworks ZIF-67, -7, -71, and -8 across various operating temperatures, achieved through complex characterization of the structural electrical, and chemical properties of the hybrid materials developed in this work.
- Establishment of the fundamental mechanisms of thermal degradation and phase transition for ZIF/MOx hybrids (ZIF-67, -7, -71, and -8 combined with ZnO:Cd) using *in situ* temperature-dependent XRD. This investigation identified thermal stability intervals and highlighted the transformation processes from ZIF-67, -7, -71, and -8 into their corresponding metal oxides (ZnO or Co_3O_4), confirming the viability of these materials for safe operation in sensory devices.
- Elucidation of the structural and physicochemical properties of ZIF-71/CuO:Al hybrid materials, correlated with the explanation of sensing mechanisms and underlying interfacial physical phenomena.
- Demonstration of the decisive role of hybridizing CuO:Al nanomaterials with ZIF-71 frameworks—forming the ZIF-71/CuO:Al structure—in enhancing dual-gas detection capabilities at different operating temperatures (200°C and 250°C). This phenomenon is attributed to the

synergistic effect between these materials; specifically, selectivity toward n-butanol at 200°C is dictated by high polarizability, while at 250°C, the heterostructure exhibits superior hydrogen selectivity due to facilitated diffusion through the framework pores.

- Substantiation of selective hydrogen gas detection using ZIF-8/CuO:Al-based hybrid materials, a process governed by the molecular sieving effect. It was established that, among the tested analytes, n-butanol exhibits increased sensitivity due to superior electronic polarizability compared to acetone or ethanol.

The scientific results were partially obtained at the Technical University of Moldova (UTM), Moldova, and at Kiel University, Germany within the framework of HORIZON SENNET project. Based on the obtained results and patent application, it is possible to further implement innovative research activities at UTM.

Approval of scientific results:

The basic results of the doctoral thesis were discussed and presented at the half-yearly and annual meetings at the Department of Microelectronics and Biomedical Engineering of Technical University of Moldova (2023-2026); periodic SENNET consortium meetings twice a year under HORIZON Europe project (2023-2026); scientific seminars of the Department of Microelectronics and Biomedical Engineering of Technical University of Moldova (2025, 2026); disseminating and presented among a wider audience in 4 national and international scientific conferences, including: International fair of innovation and creative education for youth (ICE-USV) Suceava, Romania, July 2023; MOFSIM 2024, Montpellier, France, April 2024; *IEEE 15th International Conference on "Nanomaterials: Applications & Properties",* Bratislava, Slovakia, Sept. 7-12, 2025, E-Health and Bioengineering Conference (EHB), Iasi, Romania, 2024; and International Conference on Nanotechnologies and Biomedical Engineering (ICNBME), 2025, Republic of Moldova.

The investigations in the thesis fall in the priority research and development directions of Europe including Moldova:

European Union's EU Framework Programme for Research and Innovation, Horizon Europe, under Grant Agreement No. 101072845.

Publications related to the subject of the thesis

The obtained results were published in 25 scientific publications, 14 of which are directly related to the topic of the thesis. Scientific papers on the topic of the thesis includes 1 patent application; 6 peer-reviewed articles in international journals indexed in major academic databases such as SCOPUS and Web of Science (ISI). All scientific papers were published in peer-reviewed journals with a journal impact factor exceeding 3. One article was published in journals from the National Register of specialized journals (JES- Journal of Engineering Science), and six papers/posters were presented or published in National and International Conference Proceedings. A complete list of publications is listed at the end of the thesis.

h-index=5+; i-10 index=3+. Number of citations on Google Scholar=67+; SCOPUS=45+, 12 ISI papers in Scopus, Scopus ID: 59194131400, Web of Science Researcher ID: KPA-8644-2024.

Thesis volume and structure:

A joint doctorate thesis consists of an introduction, five chapters containing 104 pages of basic text, 40 figures, 7 tables, and 37 equations, general conclusions and recommendations, 4 annexures, and bibliography with 273 references.

Keywords: MOFs, ZIFs, ZnO, synergistic, CuO, mechanism, molecular sieving effect, hybrid materials, MOF/MO, hybrids, sensor.

The basic content of the paper:

The ***Introduction*** substantiates the research topic, the problem addressed, and the importance to develop new MOF/MO heterostructured systems. It provides an analysis of the current state of research on the subject, defines the purpose and objectives of the study, and outlines its scientific novelty. The introduction also summarizes the primary scientific thesis and supporting research for defense, justifies the reliability of the results, and lists the scientific conferences attended at which the principal findings of the conducted research on the topic of thesis were disseminated through oral presentations, poster presentations, and scientific discussions, gaining approval from the scientific community.

Chapter 1 includes possible approaches to overcome the limitations of metal oxides and their applications in the sensing field by employing a variety of concepts, specifically metal-oxide/metal-organic framework or MOF/MO-based hybrid sensors. This is followed by the detailed discussion on the stability of MOFs and key factors affecting their structural phases and the corresponding structure property relationship. Theoretical concepts of characterizations tools, such as X-ray photoelectron spectroscopy, scanning electron microscopy, X-ray diffraction, and Raman spectroscopy, are also discussed in detail. In the final section of this chapter, the applications of hybrid materials for the sensing of volatile organic compounds and hydrogen are discussed thoroughly using recently published literature.

Chapter 2 outlines the experimental approaches, including the simple and cost-effective synthesis methods employed for the growth of metal oxides (ZnO, CuO, or ZnO:Cd, CuO:Al), the synthesis of zeolitic-imidazolate frameworks, and the development of corresponding MOF/MO heterostructured systems, namely ZIFs/ZnO and ZIFs/CuO-based hybrid materials. This is followed by the section including the experimental methods used for the material, thermal, sorption, and electrical characterization of the hybrid materials.

Chapter 3 presents a detailed discussion on the physicochemical properties of MOF-metal oxide (MOF/MO) systems (ZIF-8/CuO:Al) hybrid structures. This is followed by an elucidation of the surface and interfacial characteristics of the developed hybrids, as well as an evaluation of their electronic and charge-transport properties in the presence of tested gas molecules.

Figure 1(a) shows SEM images of the ZIF-8/CuO:Al-based MOF/MO hybrid structures. The SEM images of the CuO:Al film prior to the ZIF-8 coating exhibit intergranular structures and reveal triangular shaped CuO:Al grains within an approximate size range of 130 nm to 200 nm, distributed randomly without any orientation. It was observed that the CuO:Al grains are homogeneously interconnected, which can be attributed to the thermal treatment (600 °C, 60 s). Following the deposition of ZIF-8 particles on top of the CuO:Al film, the particles uniformly cover almost the whole CuO:Al surface, as shown in Figure 1(a). The SEM image reveals the rhombic-dodecahedral morphology of the ZIF-8 particles, with an estimated particle size of 70 nm. The structural features of the ZIF-8/CuO:Al hybrid structures were investigated using XRD. The XRD pattern of the investigated sample exhibits two primary peaks corresponding to CuO at 2θ angles of 38.8˚ and 35.56˚, which correspond to the (1 1 1) and (1 1 $\bar{1}$) lattice planes of the monoloclinic phase of CuO. This can be confirmed with a reference using pdf map 1526990. There are several other peaks present in the diffractogram that correspond to electrical Au connections, marked by #, as shown in Figure 1(b). The peaks corresponding to Au were confirmed using reference pdf map no. 1100138. At a lower 2θ-range from 7˚ to 32˚, multiple peaks were present which correspond to ZIF-8. The most dominant peak with highest intensity was observed at 2θ

=7.20˚, which corresponds to the (0 1 1) plane of ZIF-8. The position of all ZIF-8 peaks was confirmed using a simulated reference pattern obtained from a crystallographic information file [10]. The presence of Al is not confirmed by XRD, which can be attributed to its low concentration. No Aluminium phase was observed during XRD analysis of the ZIF-8/CuO:Al-based MOF/MO hybrid structures, though it was confirmed in the EDX composition analysis of the studied film. The vibrational states of the CuO:Al structures and the ZIF-8/CuO:Al hybrid structures were studied using the Raman spectrum (Figure 1(c)). The spectrum of the CuO:Al structures exhibit a monoclinic phase and display three Raman active modes A_g (286 cm^{-1}), B_g^1 (327 cm^{-1}), and B_g^2 (614 cm^{-1}), which can be confirmed using the reported literature [11]. Similarly, the Raman spectrum of the ZIF-8/CuO:Al hybrid structures was tested in the range of 100 to 3500 cm^{-1}. The Raman shifts observed below 200 cm^{-1} (100.4 cm^{-1}, 146.2 cm^{-1}, and 186.6 cm^{-1}) can be attributed to the lattice framework of ZIF-8. Other Raman shifts observed at higher wavenumbers, such as 296.3 cm^{-1}, 688 cm^{-1}, 1146 cm^{-1}, and 1458 cm^{-1}, can be attributed to the stretching (υ) of Zn-N bonds, the out-of-plane bending vibration of the imidazolate ring, the bending vibration of the C_5-N bond, and the methyl bending vibration, respectively. The assignment of Raman shifts can be confirmed by comparing the values for these vibrations with the reported literature [12], specifically at 278 cm^{-1}, 686 cm^{-1}, 1146 cm^{-1}, and 1458 cm^{-1}, respectively.

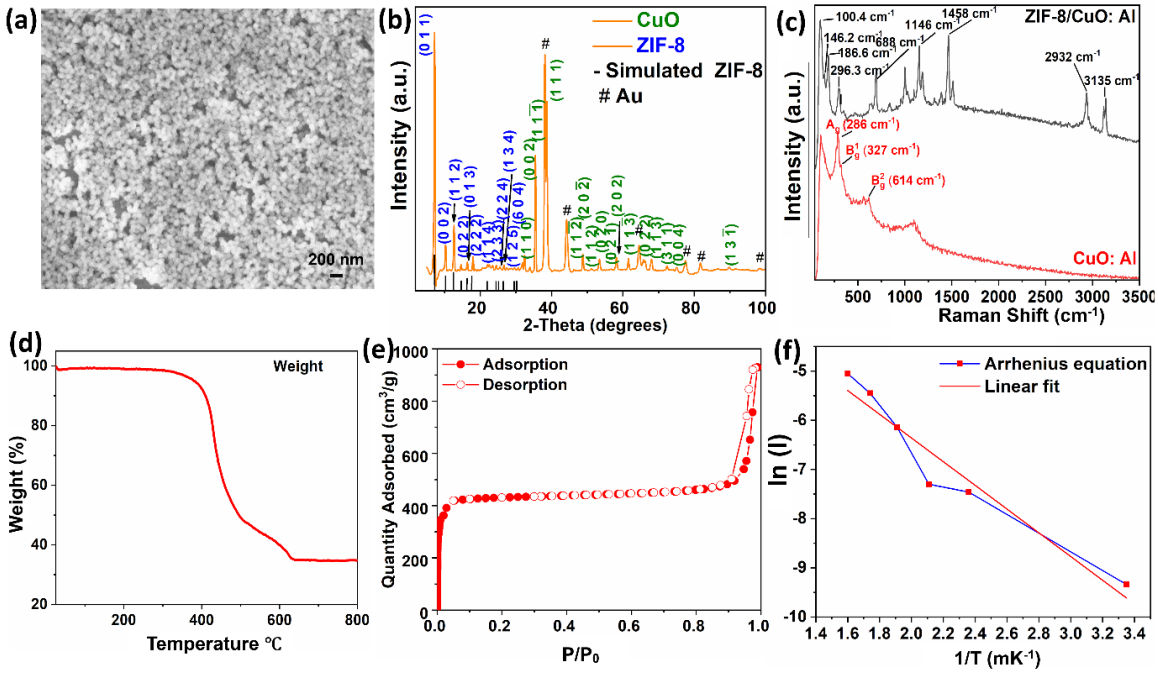

Fig. 1. (a) SEM image of the ZIF-8/CuO:Al hybrid structures. (b) XRD reflection of the ZIF-8/CuO:Al hybrid structures. (c) Raman spectra of the ZIF-8/CuO:Al and CuO:Al structures. (d) TGA profile for ZIF-8 weight decomposition in the synthetic air. (e) N_2 adsorption-desorption isotherm curve of the ZIF-8 nanoparticles. (f) Arrhenius plot of ln (I) vs 1/T with the corresponding linear fit for the calculation of activation energy of the ZIF-8/CuO:Al hybrid structures.

All the compared vibrational modes were confirmed except the one at 296.3 cm^{-1}, which shows a blue shift in the Zn-N vibrational mode. This can be attributed to the localized defects, such as missing linker or uncoordinated metal sites [13]. Two additional modes were observed at 2932 cm^{-1} and 3135 cm^{-1}. This can be attributed to the antisymmetric stretching vibration (υ)

modes of C-H in the methyl group and imidazolate ring [14,15]. All observations and the studied implications confirm that the ZIF-8 retains its structure after deposition on the CuO:Al structures.

The thermal stability tests conducted on the ZIF-8 powder under the flow of synthetic air (50 ml/min) showed negligible weight loss up to 380 ℃, indicating the absence of physiosorbed solvents or moisture content and confirming the structural integrity of the framework within the temperature range of 20 ℃ to 380 ℃ (Figure 1(d)). Subsequently, by further increasing the temperature to 640 ℃, a gradual weight loss of about 65.1% was observed, which can be attributed to the subsequent collapse of the organic framework and the decomposition of the 2-methylimidazolate linkers [16].

Furthermore, by increasing the temperature to 800 ℃, a relatively stable plateau was observed, which can be attributed to the transformation of ZIF-8 into thermally stable ZnO; this is consistent with previously reported literature [17]. To further probe the surface area of ZIF-8 nanoparticles, N_2 adsorption-desorption isotherm measurements were undertaken at 77 K, with the results depicted in Figure 1(e). Intriguingly, the ZIF-8 isotherm displayed Type-I behavior, indicating a microporous structure. The obtained BET (Brunauer-Emmet-Teller) surface area was quantified to be 1647 m^2/g, which is in good agreement with the literature [18]. To investigate the position of the defect states above the valence band, the activation energy (E_a) of the ZIF-8/CuO:Al hybrid structures was evaluated by measuring the current (I) in an ambient environment across a temperature range from room temperature (25 ℃) to 350 ℃. The slope of the linear regression can be calculated using a plot of ln(I) against 1/T (as shown in Figure 1(f)), which relates to the activation energy (E_a) divided by the Boltzmann constant (k_B) in accordance with the Arrhenius Equation [19]. The slope of the plotted curve is approximately−2.4×10^3 K, leading to an estimated activation energy of around 0.2 eV from the valence band to the defect state. This activation energy aligns with the trap levels or defect states (V_{Cu}) reported in the literature [20]. These trap levels serve as acceptor states and are integral to the p-type conductivity exhibited by CuO. Positioned just above the valence band, these shallow trap levels facilitate the thermal excitation of electrons from the valence band to the acceptor level, subsequently generating holes in the valence band that contribute to hole conduction.

XPS of the samples−CuO:Al (reference), partially covered ZIF-8/CuO:Al (low coverage), and almost fully covered ZIF-8/CuO:Al (high coverage)−was conducted to analyze the surface chemistry of all the three samples. The survey spectra of all the three samples, with their respective photoemission lines corresponding to each species, are given in Figure 2(a). Low-resolution survey scan spectra of the CuO:Al film (reference) and ZIF-8/CuO:Al hybrid structures (low coverage) exhibited a small signal from Na 1s, which may attribute to residual Na from the precursor solution (sodium thiosulfate pentahydrate) used in the synthesis process. For the CuO:Al (reference) sample, the photoelectron lines were observed from Cu, O, and C (Figure 2(a) (iii)). Moreover, the ZIF-8 covered CuO:Al (low coverage) sample exhibited Zn 2p, N 1s, and C 1s photoelectron lines (Figure 2(a) (ii)) similar to the ZIF-8/CuO:Al (high coverage) structures (Figure 2(a) (i)). Additionally, Cu related photoelectron lines were observed for the ZIF-8 covered CuO:Al (low coverage) sample due to incomplete coverage of the CuO:Al film by ZIF-8. Though, the Cu related photoelectron line was not observed in the ZIF-8/CuO:Al (high coverage) structures. In contrast, high-resolution spectra provide detailed information about chemical states and the bonding of elements by focussing on core-level electrons, which is not achievable using survey spectra alone.

High-resolution spectra for the ZIF-8/CuO:Al (high coverage) structures are illustrated in Figure 2(b-c). It demonstrated the chemical environment of core levels of present elements using deconvoluted components to derive the bonding information.

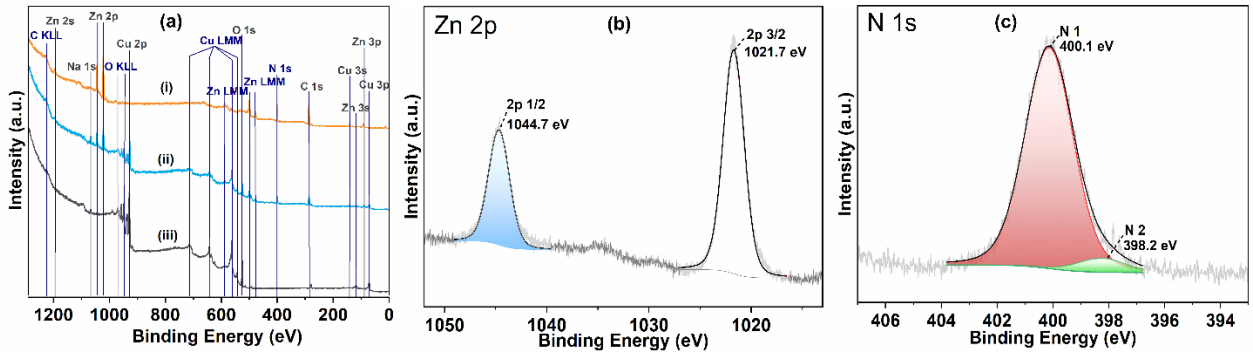

Fig. 2. XPS spectra of selected CuO:Al samples: (a) labeled survey spectra of: (i) ZIF-8/CuO:Al (high coverage), the spectrum shows the ZIF-8 characteristic XPS lines of Zn, N and C indicating complete coverage of the substrate. (ii) ZIF-8/CuO:Al (low coverage), the Cu specific substrate lines are still visible, and (iii) CuO:Al reference sample. (b – c) High-resolution spectra of the ZIF-8/CuO:Al (high coverage) sample: (b) Zn 2p and (c) N 1s.

The deconvoluted components (Zn $2p_{3/2}$ and Zn $2p_{1/2}$) of the Zn 2p spectrum (Figure 2(b)) are observed at 1021.7 eV and 1044.7 eV, respectively. The difference in the binding energies of these two lines is approximately 23 eV, which corresponds to the +2-oxidation state of Zn present in ZIF-8 [21]. Furthermore, the photoelectron line corresponding to the N 1s spectra can be deconvoluted into two components, N 1 and N 2, as shown in Figure 2(c). The more intense component, N 1, is observed at 400.1 eV, which can be assigned to the nitrogen atom linked in the imidazolate ligand to the Zn^{2+} in the ZIF-8 framework. On the other hand, the less intense component, N 2, is observed at 398.2 eV, which can be assigned to the uncoordinated 2-methyimidazolate linker.

Figure 3(a) depicts the gas sensing behavior of the bare CuO:Al and ZIF-8/CuO:Al-based MOF/MO hybrid sensor toward 100 ppm of a series of relevant reducing gases: hydrogen, n-butanol, 2-propanol, ethanol, acetone, and ammonia, at operating temperatures ranging from 250 to 350 °C. By increasing the temperature from 250 °C to 350 °C, the hydrogen response steadily increased, a maximum response of 170% at 350°C was observed. Conversely, other gases exhibited bell-shaped response curves with maxima at 250 °C, followed by a decline in sensing response at higher temperatures due to accelerated desorption [22]. Among the ABE (acetone-butanol-ethanol) molecules, the strongest response was observed for n-butanol across all tested operating temperatures, indicating a greater adsorption affinity than acetone and ethanol, in accordance with competitive adsorption isotherms in ternary ABE systems [23]. The prepared sensor demonstrated approximately 1.3- and 1.6-times higher selectivity toward n-butanol relative to ethanol and acetone, respectively. The hydrogen response at 350 °C exceeded those of the other gases by a factor greater than four. The theoretical lowest detection limit ($LDL = (3 \times rms_{noise})/slope\ of\ linear\ fit$) of the sensor is defined as the minimal concentration of an analyte that can be reliably detected. Figure 3(b) illustrates the relationship between the gas sensing response (S) and hydrogen concentration.

The rms_{noise} is determined to be 0.18%, and the slope (s) of the sensing response as a function of analyte concentration is 1.34%/ppm. Consequently, the *LDL* for the ZIF-8/CuO:Al-based MOF/MO hybrid sensor is approximately 402 ppb.

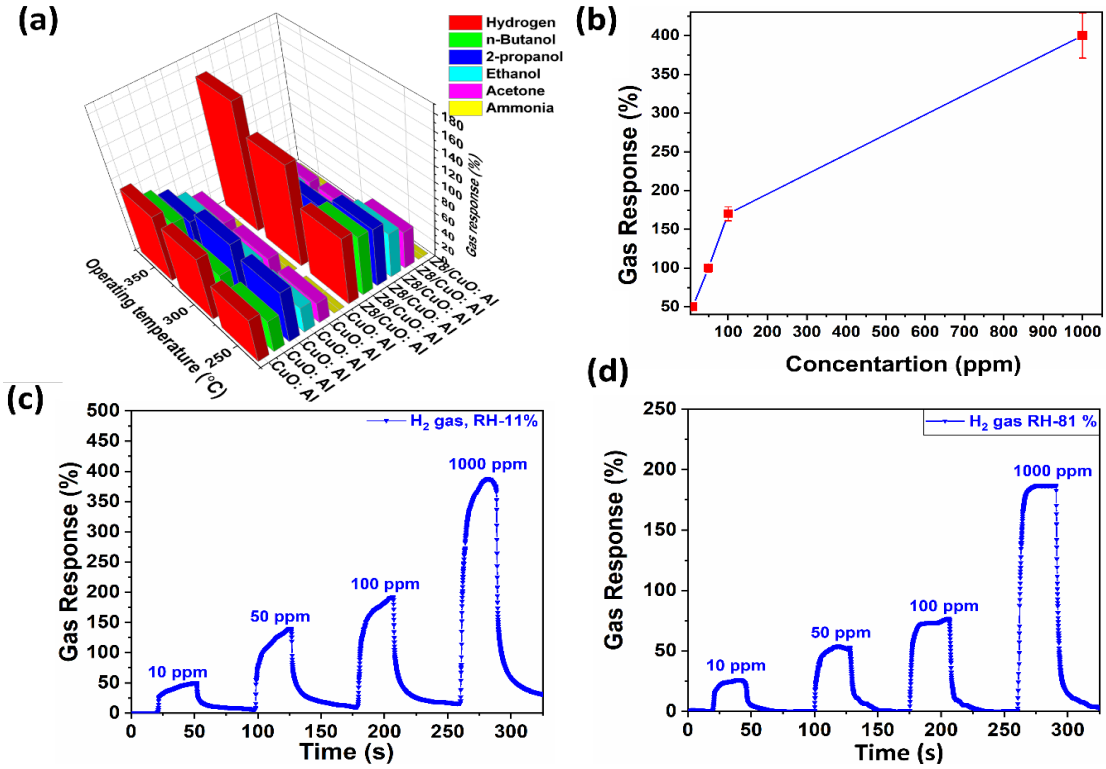

Fig. 3. (a) Comparative gas sensing characteristics of the bare CuO:Al and ZIF-8/CuO:Al-based hybrid sensors at different operating temperatures. (b) Sensing response (%) of the ZIF-8/CuO:Al hybrid sensor as a function of the hydrogen concentration. Gas response of the ZIF-8/CuO:Al based hybrid sensor to different hydrogen concentrations and RH values (c) RH 11%, and (d) RH 81%.

The gas response characteristics of the ZIF-8/CuO:Al hybrid structures were evaluated upon exposure to varying hydrogen concentrations ranging from 10 to 1000 ppm, under operating conditions of RH 11% at 350°C (Figure 3(c)). The sensor demonstrates the capability to detect hydrogen concentrations as low as 10 ppm, yielding a response of approximately 50%. As the hydrogen concentration increases, a corresponding rise in response is observed, attaining nearly 400% at 1000 ppm. Furthermore, an increase in relative humidity to 81% results in a decrease in the gas sensing response to about 75% at a concentration of 100 ppm, as depicted in Figure 3(d).

The hybrid structures were employed in gas-sensing studies of the target analytes, and the corresponding sensing mechanisms were discussed based on the molecular sieving effect. The gas sensing mechanism and selectivity for target analytes can be understood using different models. The high selectivity for hydrogen can be attributed to the molecular sieving effect, which allows small hydrogen molcules to pass through the pores of ZIF-8. The presence of the ZIF-8 layer enabled the diffusion of the target analytes through the pore via the Knudsen diffusion regime. Upon reaching to the ZIF-8 and CuO:Al interface, the sensing mechanism can be understood using the ionosorption model.

Chapter 4 presents the physical and chemical properties of ZIF-71/CuO:Al-based MOF/MO hybrid structures, followed by an analysis of the thermal and sorption properties of the

ZIF-71 particles. Initial investigations into the surface morphology of the CuO:Al structures and the ZIF-71/CuO:Al composite-based hybrid structures were conducted using SEM. The SEM image in Figure 4(a) revealed a uniform covering of ZIF-71 patticles on the intergranular structures of the CuO:Al structures covering the entire glass slide substrate.

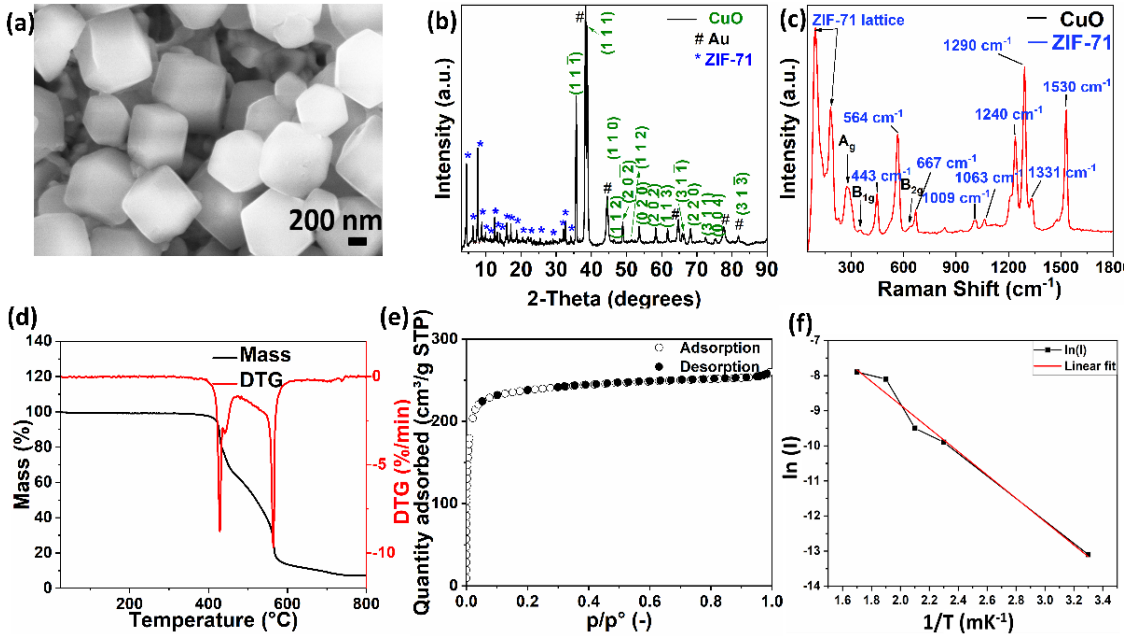

Fig. 4. (a) SEM image of the ZIF-71/CuO:Al structures. (b) XRD reflections of the ZIF-71/CuO:Al structures with Au IDEs. (c) Raman spectra the ZIF-71/CuO:Al structures. (d) Thermal stability test of the ZIF-71/CuO:Al structures using TGA. (e) Nitrogen-sorption isotherm of the ZIF-71/CuO:Al structures. (f) The Arrhenius plot of ln (I) vs 1/T for the calculation of activation energy.

CuO:Al grains exhibited random orientations, indicative of isotropic growth during the annealing process [24]. In addition, SEM analysis of the ZIF-71/CuO:Al-based MOF/MO hybrid structures displayed almost complete coverage of the CuO:Al surface with ZIF-71 particles, which exhibited a rhombic dodecahedron morphology following the deposition of 100 µL of the ZIF-71 dispersion. This image facilitates a preliminary particle size assessment, estimating sizes in the range of 500 nm to 750 nm. The labelled XRD pattern of the ZIF-71/CuO:Al-based MOF/MO hybrid structures is depicted in Figure 4(b). Prominent reflections of CuO were detected at 38.83˚ and 35.67˚, corresponding to the (1 1 1) and (1 1 $\bar{1}$) lattice planes of CuO (PDF card no. 1526990). Well-resolved Bragg reflections throughout the measurement range of 2θ (2˚to 90˚) were labelled, which can be attributed to CuO (PDF card no. 1526990), Au (PDF card no. 1100138), and ZIF-71 [25]. Additional significant reflections associated with Au, evident in Figure 4(b), arise from the Au interdigitated electrodes (IDEs) utilized for electrical characterization. Figure 4(c) presents the Raman spectrum of the ZIF-71/CuO:Al film, revealing several characteristic peaks that indicate the structural integrity of the ZIF-71 framework is preserved. Peaks below 200 cm^{-1} are assigned to the ZIF-71 lattice framework, aligning with prior studies [26]. The peak at 443 cm^{-1} corresponds to the stretching vibration of the Zn-N bond [27]. Peaks at 667 cm^{-1}, 1009 cm^{-1}, and 1063 cm^{-1} are associated with the in-plane deformation of the imidazolate ligand linker rings, as previously reported [28]. In addition, peaks near 295 cm^{-1}, 343 cm^{-1}, and 629 cm^{-1} correspond to the A_g, B_g^1, and B_g^2 vibrational modes of the CuO film, respectively [29]. The Raman bands at 1290 cm^{-1} and

1240 cm^{-1} are due to C-H vibrations, while the peak at 1331 cm^{-1} is associated with C=N stretching within the imidazolate ring, as verified by earlier investigations [30].

The thermal stability of ZIF-71 particles was assessed using TGA. The weight loss (TG) and the DTG are illustrated in Figure 4(d), demonstrating negligible weight loss up to 400°C, confirming that ZIF-71 is thermally stable in that temperature range. A significant weight loss around 415°C is attributed to the decomposition of the ZIF-71 structure, leading to the formation of ZnO. The total weight loss observed from 400°C to 700°C was 88%, exceeding the theoretical mass loss of 76% expected when ZIF-71 converts to ZnO. This discrepancy between theoretical and experimental weight loss may be explained by the presence of 4,5-dichloroimidazole linkers coordinated to terminal zinc atoms at the crystal surface [31]. The surface area and pore size distribution of the ZIF-71 particles were analyzed by measuring a nitrogen adsorption-desorption isotherm at 77 K. The isotherm presented in Figure 4(e) displays a distinct inflection at low relative pressures (P/Po < 0.1), characteristic of a Type I isotherm according to IUPAC classification, confirming a microporous structure with pore diameters less than 2 nm. Figure 4.2(d) illustrates the BET pore size distribution, revealing a calculated surface area of 969.9 ± 6.3 m^2/g with an average pore size of 16.3 Å, which is in accordance with literature [32].

The location of the defect states can be determined using the Arrhenius plot by calculating the corresponding activation energy (E_a). The activation energy (E_a) of the CuO:Al film was assessed by plotting the logarithmic current (ln I) measurements in relation to the inverse of the corresponding temperature (1/T) (Figure 4(f)). The slope of the plotted curve comes out to be approximately 3.32×10^3 K. The activation energy (E_a) was calculated to be approximately 0.28 eV. The determined activation energy (E_a) corresponds to defect level or hole trap states (V_{Cu}) [33]. Specifically, it corresponds to the copper shallow acceptor states, compared to deep acceptor states observed in other metal oxides (e.g., MgO) [34].

The surface chemistry of the ZIF-71/CuO:Al structures, including elemental chemical states and bonding environments, was characterized using XPS. The survey spectrum in Figure 5(a) reveals signals attributed to carbon and nitrogen from imidazolate units, zinc cations, and chlorine anions from the organic ligand.

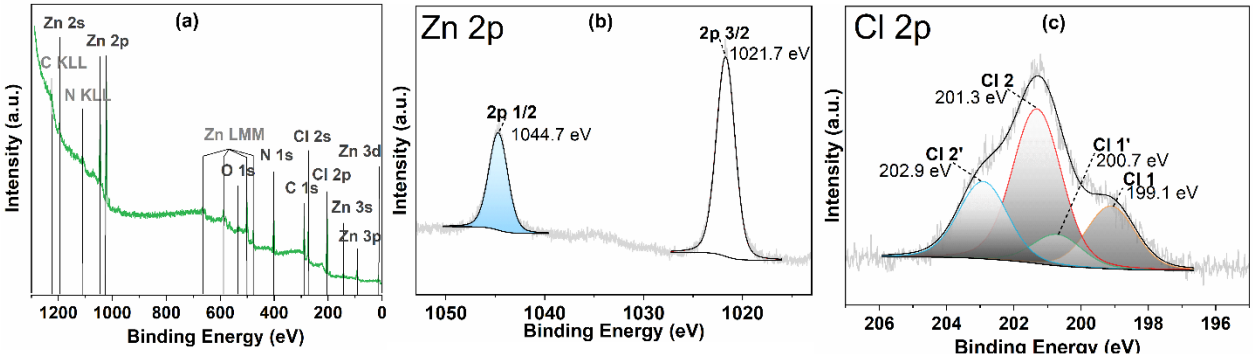

Fig. 5. XPS spectra of the ZIF-71/CuO:Al structures: (a) survey spectra showing XPS lines of all elements present. High-resolution (b) Zn 2p region. (c) Cl 2p region.

The absence of copper and aluminum signals confirms near-complete surface coverage by ZIF-71. A minor O 1s peak suggests minimal surface oxidation, despite the sample's prolonged air storage prior to measurement. High-resolution XPS spectra, presented in Figures 5(b)–(c), provide detailed insights. The Zn 2p spectrum (Figure 5(b)) exhibits characteristic spin-orbit split peaks at

1021.7 eV (Zn 2p3/2) and 1044.7 eV (Zn 2p1/2) with a 23.0 eV splitting [35], indicative of a single zinc species. The higher binding energy component aligns with previous synchrotron X-ray studies revealing ZIF-71 degradation [36], while the Zn 2p remained stable, validating its role as a binding energy reference. The Cl 2p region (Figure 5(c)) displays four peaks corresponding to two spin-orbit doublets: Cl 2 and Cl 2′ at 201.3 and 202.9 eV assigned to C-Cl bonds [37], and Cl 1 and Cl 1′ at 199.1 and 200.7 eV [36], respectively, associated with Zn-Cl bonds formed during X-ray-induced degradation [36]. The C-Cl doublets constitute 71% of Cl intensity, whereas Zn-Cl degradation products represent 21%. The C 1 species at 285.2 eV is thus linked to degradation products characterized by C-C or C-H bonds not bonded to chlorine or nitrogen.

The ZIF-71/CuO:Al-based MOF/MO hybrid material demonstrates a synergistic effect of its individual components, enabling effective sensing of n-butanol and hydrogen at different operating temperatures. Comparative gas sensing results at low (10%) and high (50%) RH, measured 21 days after the initial measurements, are demonstrated in Figures 6(a) and (b).

Figure 6(a) presents the gas sensing response (*S*) of the ZIF-71/CuO:Al hybrid sensor at 10% RH, demonstrating a maximum response for n-butanol at 200°C, whereas at 250°C, all test gases exhibited enhanced responses, especially hydrogen. Figure 6(b) illustrates the sensor's response to various target analytes at 50% relative humidity. As the temperature increased from 200°C to 250°C, the sensor demonstrated increased selectivity toward 100 ppm hydrogen gas. Comparing Figures 6(a) and 6(b) highlights the effect of humidity: increasing RH from 10% to 50% substantially degraded the sensor's response to n-butanol across all operating temperatures. This behavior is attributed to incomplete ZIF-71 surface coverage and competitive adsorption between hydroxyl ions and oxygen species.

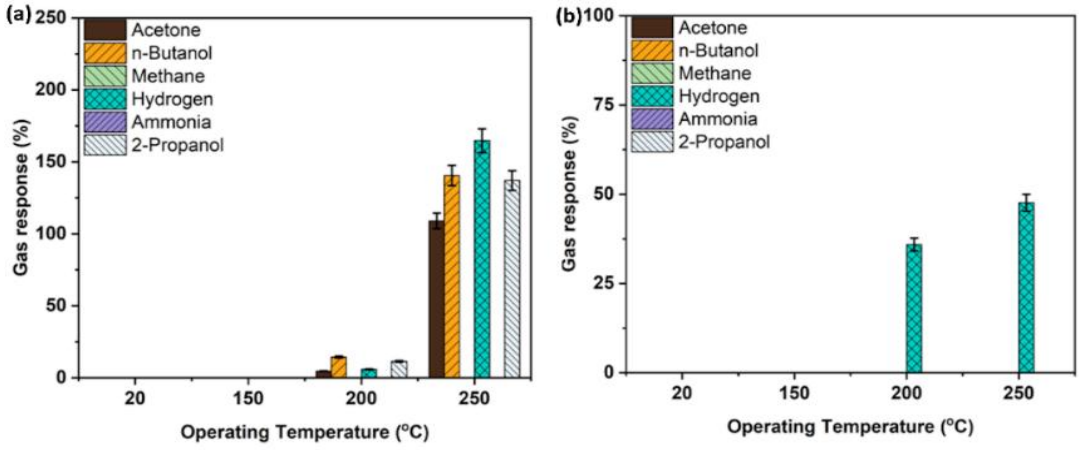

Fig. 6. Gas response to a series of gases with concentration of 100 ppm at different operating temperature for the ZIF-71/CuO:Al hybrid sensor at (a) low relative humidty (10%) and (b) high relative humidty (50%).

The corresponding sensing mechanisms, based on ionosorption and transport physics, are discussed to explain the observed results and the underlying physical processes. The adsorption of oxygen ions on the sensor surface via surface traps creates a high potential barrier and a hole accumulation layer, causing upward band bending and a consequent decrease in the resistance of the accumulation layer. Upon exposure to n-butanol at 200°C, the corresponding adsorbed oxygen species react with the analyte, releasing electrons that recombine with holes in the bulk material. This recombination leads to a decrease in the hole concentration in the accumulation layer,

resulting in downward band bending ($q\Delta V = \Delta\Phi$) and an increase in the resistance of the accumulation layer [8].

According to the diffusion model, the Knudsen number (K_n) was calculated for n-butanol and hydrogen at two different operating temperatures (200°C and 250°C) where temperature-dependent selectivity was observed. The calculated values at 200 °C (n-butanol: 122 and hydrogen: 267) and 250 °C (n-butanol: 135 and hydrogen: 294) clearly indicate that both gases at both temperatures fall within the Knudsen diffusion regime ($K_n > 10$). However, the ZIF-71 film is not entirely free of pinhole defects. Transport through grain boundaries and other minor defects may locally decrease the Knudsen number (K_n) in certain areas. Therefore, it can be concluded that the intrinsic transport of n-butanol and hydrogen through the ZIF-71 pores at both temperatures predominantly occurs via Knudsen diffusion, although localized contributions from transitional or molecular diffusion may arise at grain boundaries and defects. The molecular sizes of n-butanol, acetone, and 2-propanol are comparable to the pore size, facilitating access via a molecular sieving effect. Though, n-butanol shows a stronger affinity for ZIF-71 adsorption sites compared to smaller molecules like acetone and 2-propanol due to its longer carbon chain, which enhances van der Waals interactions within the ZIF-71 framework [38].

Chapter 5 is dedicated to a comprehensive discussion of the material, physicochemical, and sensing properties of ZIFs/ZnO-based hybrid structures. Figure 7(a) to (d) illustrate the SEM images of four hybrid sensors, including ZIF-67/ZnO, ZIF-7/ZnO, ZIF-71/ZnO, and ZIF-8/ZnO-based hybrid structures, respectively.

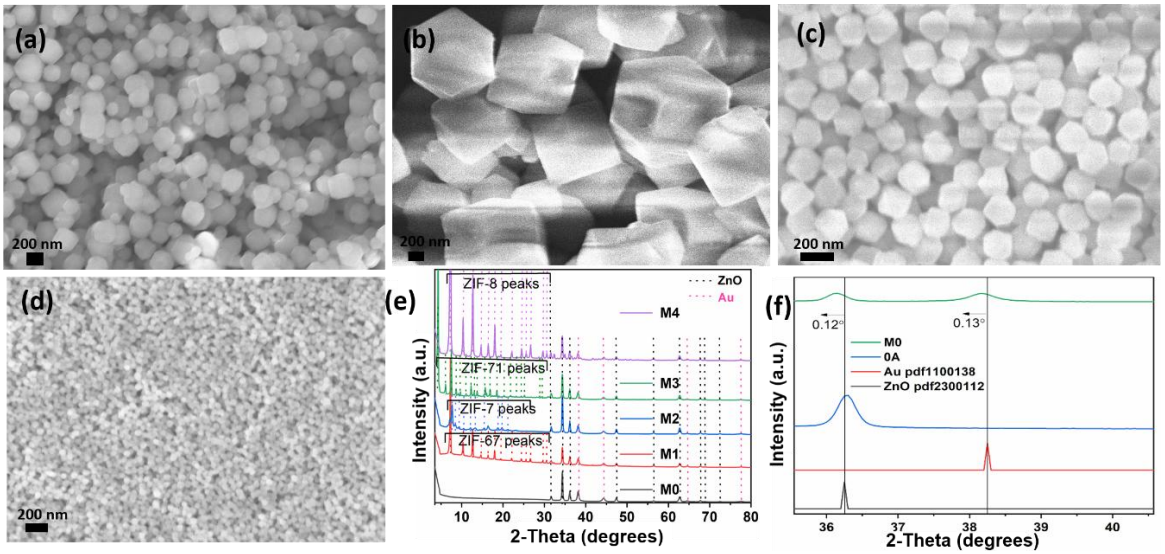

Fig. 7. SEM micrographs of (a) ZIF-67/ZnO, (b) ZIF-7/ZnO, (c) ZIF-71/ZnO, and (d) ZIF-8/ZnO-based hybrid structures. XRD of series of samples: (e) M0, M1, M2, M3, and M4. (f) comparison of 0A and M0 sample to show the crystallographic peak shift due to Cd doping.

The surface morphology of the hybrid structures was investigated using SEM. SEM micrographs of the ZIF-67/ZnO and ZIF-7/ZnO structures revealed a dodecahedral morphology with ZIF particle sizes of 200 nm for both ZIFs in their respective images (Figures 7(a) and (b)). Furthermore, SEM micrographs corresponding to ZIF-71/ZnO and ZIF-8/ZnO structures revealed particle sizes in the range of 500 to 700 nm and approximately 70 nm, respectively (Figures 7(c)

and (d)). Moreover, the ZIF-71 and ZIF-8 particles also exhibited a dodecahedral morphology. To study the structural properties of the prepared samples, an XRD investigation was carried out.

The discussion on two series requires repeating similar names multiple times. To avoid this repetition, codification scheme is proposed: ZnO (0A), ZIF-67/ZnO (1A), ZIF-7/ZnO (2A), ZIF-71/ZnO (3A), ZIF-8/ZnO (4A), Cd-doped ZnO (M0), ZIF-67/Cd-doped ZnO (M1), ZIF-7/Cd-doped ZnO (M2), ZIF-71/Cd-doped ZnO (M3), and ZIF-8/Cd-doped ZnO (M4).

The structural features of the sample series were examined using XRD. Structural investigations of all the studied hybrid structures elucidate distinct diffraction peaks indicating high crystallinity (Figure 7(e) and (f)). The XRD pattern corresponding to ZnO:Cd matches the hexagonal wurtzite structure (PDF 2300112). In ZnO:Cd, the dominant reflection was observed at 34.34˚, which correspond to the (0 0 2) plane, indicating preferential growth along the c-axis, perpendicular to the substrate. The presence of highly crystalline reflections, corresponding to ZIF-67 [39], ZIF-7 [40], ZIF-71 [41], and ZIF-8 [42], has been marked, as shown in Figure 7(e). It was revealed that the dominant reflection from all ZIFs corresponds to the {1 1 0} family of planes. By comparing the XRD reflections of 0A and M0 samples, a clear shift of approximately 0.12˚can be observed for the (1 0 1) plane (Figure 7(f)). Au IDEs were used for making electrical contacts, and their observed reflections matched those of Au (PDF 1100138). Similarly, after Cd doping, a shift in the Au (1 1 1) reflection to lower 2θ values was observed (Figure 7(f)). Cd incorporation leads to shift in lower 2θ values has also been reported in previous studies [43]. This can be attributed to the larger ionic radius of Cd^{2+} (~0.92 Å) substituting for Zn^{2+} ions (~0.74 Å) at crystallographic positions [44].

Particular emphasis is placed on temperature-dependent *in-situ* X-ray diffraction analysis of ZIF-n (n=67, 7, 71, and 8), which provided insights into thermal degradation, phase transition, and structural transformations of ZIFs into the corresponding metal oxides. This correlates the structure-property-performance relationships in the resulting hybrid materials. An *In-situ* temperature dependent XRD measurements were carried within a temperature range of 30 ℃ to ≥500 ℃ for all studied ZIF-based samples (Figure 8(a)-(f)).

For ZIF-67, by spanning the temperature increment from 30 ℃ to 250 ℃, it was observed that the spectral intensity of XRD reflections diminished, indicating a loss in crystallinity of the ZIF-67 framework (Figure 8(a)), which can be attributed to thermal stress. By increasing the temperature to higher temperatures (500 ℃), complete transformation of ZIF-67 framework into Co_3O_4 was observed. At 250 ℃, the coexistence of both ZIF-67 and transformed Co_3O_4 reflections was noted. XRD investigations on ZIF-7 demonstrated a phase change as the temperature increased from 50 to 100 ℃. At lower temperatures (30 ℃ and 50 ℃), the diffraction reflections correspond to phase I. At 100 ℃, significant changes were observed: an emerging reflection at 2θ = 6.77˚accompanying by a slight shift in some other peaks at lower angles (Figure 8(b)). These changes result in the transformation of the initial phase (phase-I) into phase-II, which may be attributed to the release of synthesis or dispersion solvent molecules (DMF or methanol), followed by the rearrangement of the ZIF-7 framework. A further increase in temperature to 325 ℃ resulted in the loss of diffraction intensity for the main reflection at 2θ (8.36˚), as shown in Figure 8(c). This revealed slow decomposition and a loss of crystallinity in phase-II, attributed to the thermal stress. Transitioning from phase-I to phase-II resulted in a loss of symmetry in the crystal structure. At 325 ℃ or higher, an incremental loss of long-range order of Miller indices (h k l) was observed at 2θ > 10˚. Moreover, the transformation of ZIF-7 into ZnO began at 375 ℃, where both phases

co-exist, followed by complete dissociation of the ZIF-7 framework at 400 ℃. The effect of increasing temperature was also clearly observed in the diffraction intensity of ZIF-71 (Figure 8(d)). From 30 ℃ to 325 ℃, gradual loss in crystallinity and sluggish decomposition of the ZIF-71 framework occurred due to the thermal stress. Increasing the temperature to 350 ℃ led to the emergence of ZnO reflections and the almost diminished intensity of ZIF-71 reflections. For ZIF-8, a gradual loss in diffraction intensity and sluggish decomposition were observed from 30 ℃ to 300 ℃. At 325 ℃, an incremental loss of long-range order for Miller indices above 13˚(2θ) was observed, along with the coexistence of ZIF-8 and ZnO reflections. Additionally, the increase in temperature from 30℃ to 325℃ affected the FWHM of the XRD peaks. Complete transformation of ZIF-8 into ZnO was observed at 350 ℃; further heating to 500 ℃ improved crystallinity and decreased peak broadening. Furthermore, the temperature increases to 325 ℃ caused a slight shift (~0.12˚) in diffraction peaks toward higher 2θ angles (Figure 8(e)), indicating shrinkage of the ZIF-8 framework due to the release of guest molecules. Heating from 400 ℃ to 800 ℃ shifted the XRD peaks by 0.2˚ toward higher 2θ angles (Figure 8(f)). *In-situ* temperature-dependent XRD results revealed that the ZIF-8 framework deteriorates at a higher temperature (325 ℃) compared to ZIF-67 (250 ℃), which cannot be understood only by considering the bond energy concept alone. Diving deeper into the realm of coordination chemistry of Co and Zn with N provides some significant insights: Zn ($3d_{10}4s_2$) has a completely filled outermost shell, whereas Co ($3d_74s_2$) is incomplete. Thus, Zn forms saturated coordination with N, whereas Co forms unsaturated coordination, making it prone to oxygenation. This results in the faster thermal decomposition of ZIF-67 at 250 ℃. A fundamental understanding of these mechanisms confirmed that ZIF-67, ZIF-7, ZIF-71, and ZIF-8 are stable up to 250 ℃, 375 ℃, 350 ℃, and 350 ℃, respectively.

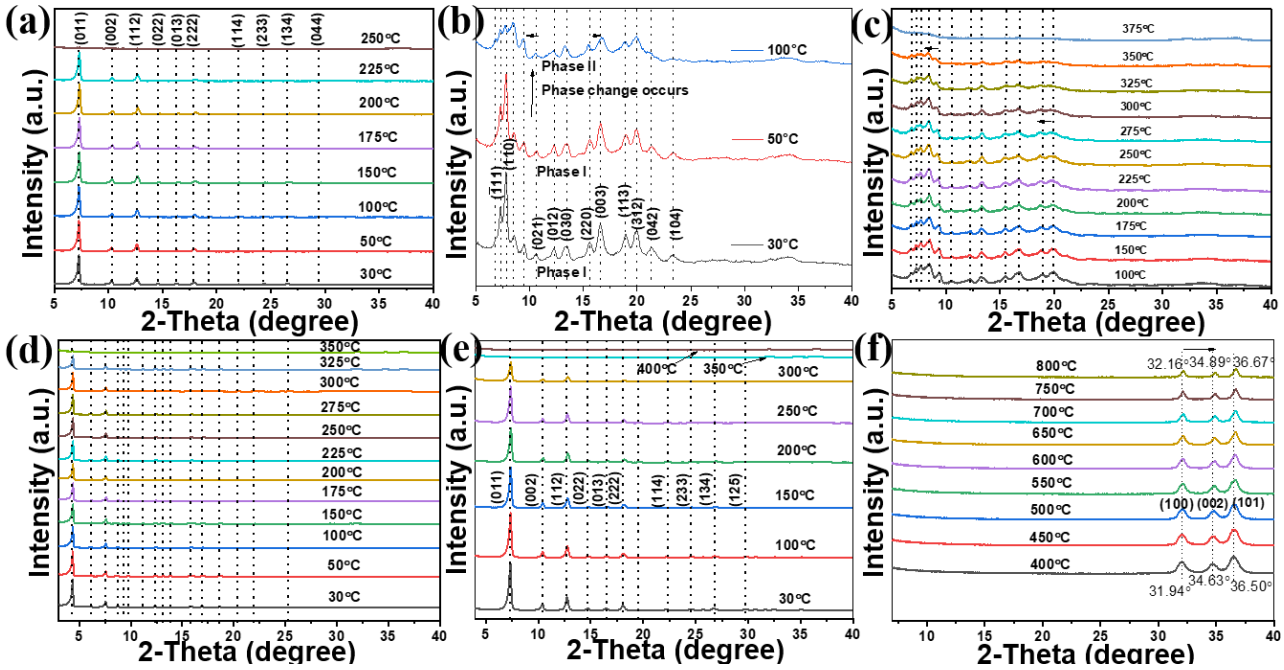

Fig. 8. *In-situ* temperature dependent XRD study of all the four studied ZIFs: (a) ZIF-67, (b, c) ZIF-7, (d) ZIF-71, and (e, f) ZIF-8 particles.

The Raman spectra of the ZnO based samples (1A, 2A, 3A, and 4A) with four different ZIF coatings−ZIF-n (n=67, 7, 71, and 8), respectively−were investigated in detail. In sample 1A, the vibrational modes corresponding to the ZnO and ZIF-67 framework were observed (Figure

9(a)). Specifically, vibrational modes corresponding to the ZIF-67 framework were observed at 120, 171, 256, 281, 419, 679, 1110, and 1452 cm^{-1}. These correspond to its lattice vibrations, N-Co-N bending, linker vibrations, N-Co-N bending, N-Co-N bending, linker vibrations, υ-C_5-N stretching, and methyl bending vibrations, respectively, as corroborated by previously published results [15]. For sample 2A, the vibrational modes corresponding to the ZIF-7 framework were observed at 83.9, 121.6, 547.3, 644.3, and 1345 cm^{-1} (Figure 9(b)).

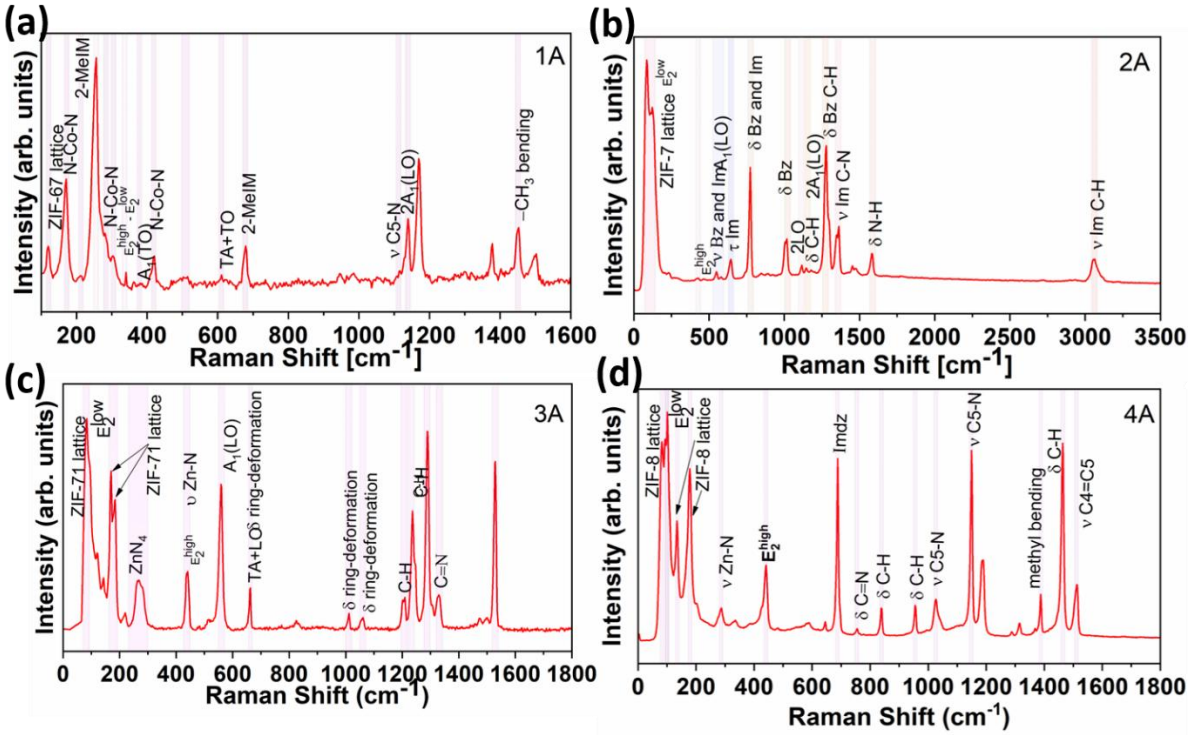

Fig. 9. Raman spectra of the ZIF/ZnO samples: (a) 1A, (b) 2A, (c) 3A, and (d) 4A.

These are associated with the lattice framework (83.9 and 121.6 cm^{-1}) and bond stretching in the benzimidazolate (Bz) and imidazolate (Im) linker rings (547.3 and 1345 cm^{-1}), respectively [45]. Furthermore, the phonon modes corresponding to the ZIF-71 framework were observed at 84, 169.7, 183.9, 266.6, 422.3, 660.9, 1011.3, 1054.9, 1209.4, 1236, 1288, and 1328 cm^{-1} (Figure 9(c)). These modes are associated with the ZIF-71 lattice framework (84, 169.7, and 183.9 cm^{-1}) [26], the tetrahedra configuration of ZnN_4 (266.6 cm^{-1}) [26], Zn-N bond stretching (422.3 cm^{-1}) [26], in-plane dichloroimidazolate ring deformation (660.9, 1011.3, and 1054.9 cm^{-1}) [28], and C-H and C=N bending and stretching vibrations (1209.4, 1236, 1288, and 1328 cm^{-1}) [26], respectively. Moreover, the phonon modes corresponding to the ZIF-8 lattice framework were observed at 82, 135, and 179 cm^{-1}, which corroborated well with prior published results [15]. These observed modes can be attributed to structural changes and phase transitions in the ZIF-8 lattice framework [15]. Other phonon modes were observed at 285, 1025, 1146, and 1512 cm^{-1}, which can be assigned to the stretching of Zn-N, C_5-N, C_5-N, and C_4=C_5 in the imidazolate ring, respectively [12]. Rest of the observed phonon modes correspond to in-plane or out-of-plane bending vibrations (Figure 9(d)). A comparative study of sample M1 and 1A (1C) (Figure 10(a)) demonstrated the Raman shift spectral range of both samples within a range 0-1600 cm^{-1}. A clear shift in the corresponding phonon modes can be attributed to the large ionic radius of Cd compared to Zn ion in the ZnO lattice, leading to increased lattice stress, this provides insights into electron-phonon interactions.

The thermal stability profile was evaluated for all four ZIFs using TGA (Figure 10(b)). It demonstrated the thermal stability of ZIF-n (n=67, 7, 71, and 8) particles until reaching 330, 480, 410, and 370 ℃, respectively, at which point weight reduction increases up to 360, 540, 580, and 610 ℃.

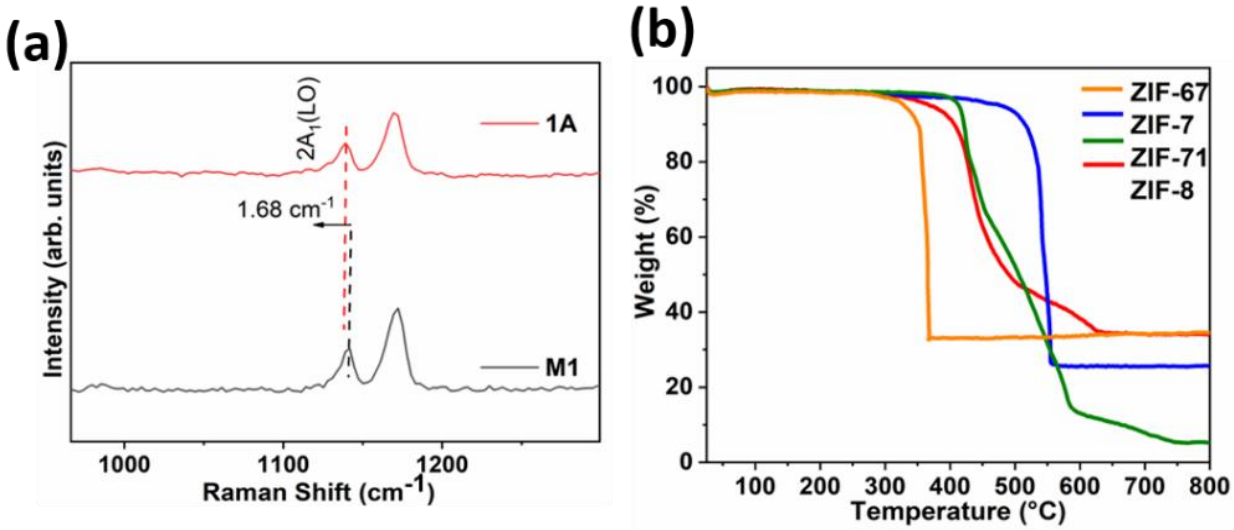

Fig. 10. (a) Comparative study of sample M1 and 1A and (b) Thermal stability test of all four ZIFs using TGA.

At a final temperature of 800 ℃, the remaining mass residues were 34.5%, 34.1%, and 25.6% for ZIF-67, ZIF-7, and ZIF-8, respectively. These values corroborate the theoretical residue masses of 36.3%, 35.4%, and 25.4%, which correspond to the formation of the respective metal oxides, Co_3O_4 for ZIF-67 and ZnO for ZIF-7 and ZIF-8. On the contrary, the residue mass for ZIF-71 was observed to be 5.2%, which is significantly less than the theoretical mass residue of 23.4%.

To examine the surface chemistry of the developed ZIF-coated Cd-doped ZnO-based hybrid structures, XPS measurements–a surface-sensitive technique–were performed on the M1 – M4 sample set. As inferred from the survey scan spectra of the measured samples (Figure 11), the photoelectron lines and Auger electron peaks were labelled from the core-levels and LMM levels, respectively. All sample spectrum contain core-levels lines, such as C 1s, N 1s, O 1s, and Zn 2p, confirming the presence of C, N, O, and Zn in each measured sample. Moreover, the presence of Co 2p core level was observed in the M1 sample, which correspond to the central metal of ZIF-67 [46]. In sample M3, the presence of Cl was confirmed by two distinct photoelectron lines from Cl 2s and Cl 2p, associated with the presence of dichloroimidazolate linker in the ZIF-71 framework [35]. The presence of the Zn 2p core level in samples M2-M4 was expected due to the presence of Zn as the central metal in the framework [47]. However, Zn 2p core levels (low intensity) were also observed in sample M1; these are not present in ZIF-67 but originate from the ZnO. This indicates that the ZIF-67 does not cover the whole ZnO surface, which can be attributed to inhomogeneous thickness and the presence of potential voids resulted from the drop-casting approach. Moreover, the influence of substrate was also observed in sample M3, where a distinct side peak of the Zn 2p signal was noted, associated with the ZnO surface at a different surface charge. The effect of doping–i.e. the presence of Cd–was not observed in the survey spectra of any sample due to the low doping concentration in ZnO.

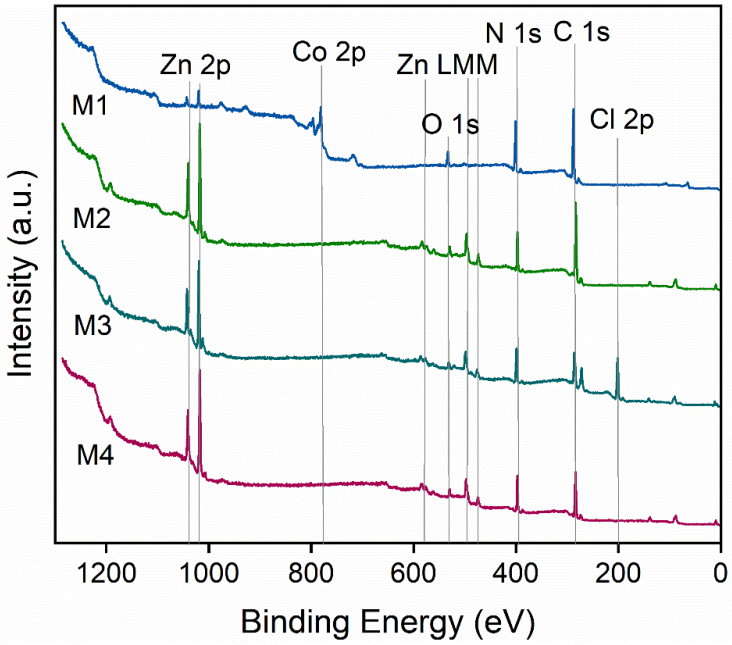

Fig. 11. XPS survey spectra of ZIF-coated Cd-doped ZnO samples: M1 (ZIF-67), M2 (ZIF-7), M3 (ZIF-71), and M4 (ZIF-8).

Gas-sensing results were evaluated for all merasured samples in series 1A-4A (Figure 12(a)-(d)) and sample series M1-M4.

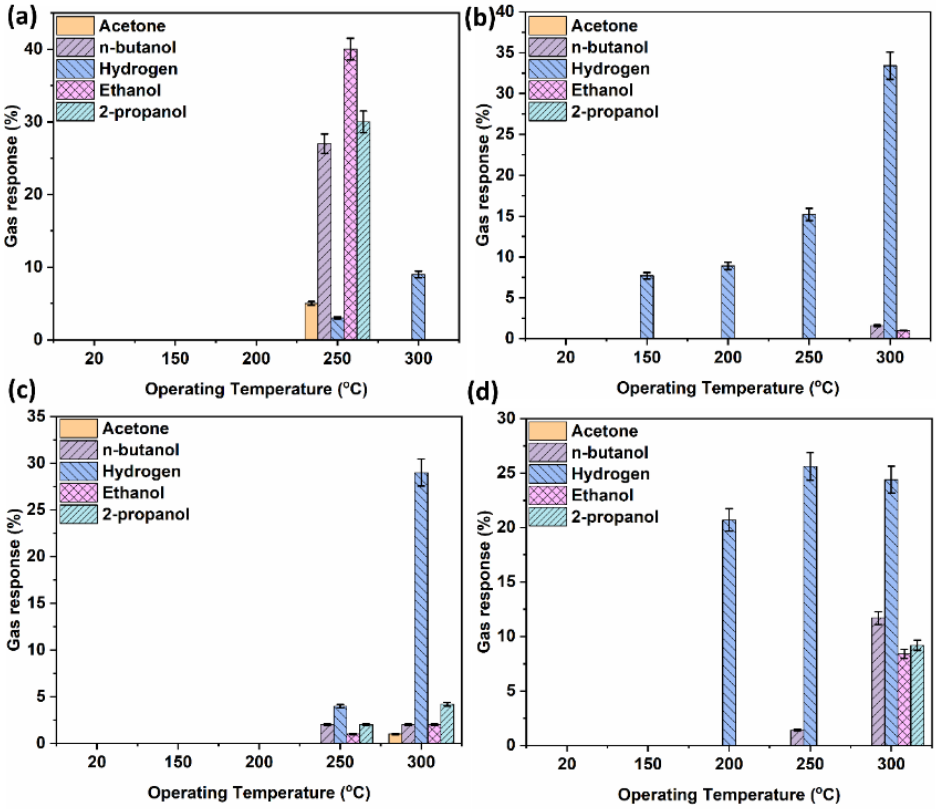

Fig. 12. Gas sensing results of sample series (a) 1A, (b) 2A, (c) 3A, and (d) 4A.

The gas-sensing results of the developed hybrid sensors exhibited appreciable selectivity for ethanol (using sample 1A), 2-propanol and n-butanol (using samples M1, 1A, 4A, M2, and M4), and hydrogen (using samples 2A, 3A, 4A, M2, M3, and M4). The effect of Cd doping was

observed in the gas sensing results; samples in the M-series exhibited selectivity toward n-butanol and hydrogen at 150 and 300 ℃, respectively. The transport mechanism demonstrated that predominantly passage of tested analytes followed Knudsen diffusion regime, although due to the presence of pinholes and grain boundaries, molecular flow and transitional flow also contributed in localized regions.

This chapter also addresses the application of these hybrid structures in gas-sensing devices and explains the corresponding sensing mechanisms using appropriate models, including the p-n heterostructure effect, ionosorption model, transport physics, and others.

It was observed that, for all the studied samples, sensing responses occured in the temperature range of 150-300 ℃, which clearly indicated the dominance of monoionic oxygen species (O^-) [48]. The trapping of electrons from the ZnO conduction band by adsorbed monoionic oxygen species resulted in an increase in the surface work function and upward band bending in ZnO (Figure 13). This, in turn, led to an increase in the electrical resistance of ZnO. Following exposure to reducing gases (n-butanol, ethanol, 2-propanol, hydrogen, and acetone), the trapped electrons were released back into the ZnO conduction band [8], contributing to a decrease in the electrical resistance of ZnO. This led to a reduction of the upward band bending ($q\Delta V = qV_1 - qV_2$), and the EDL became thinner.

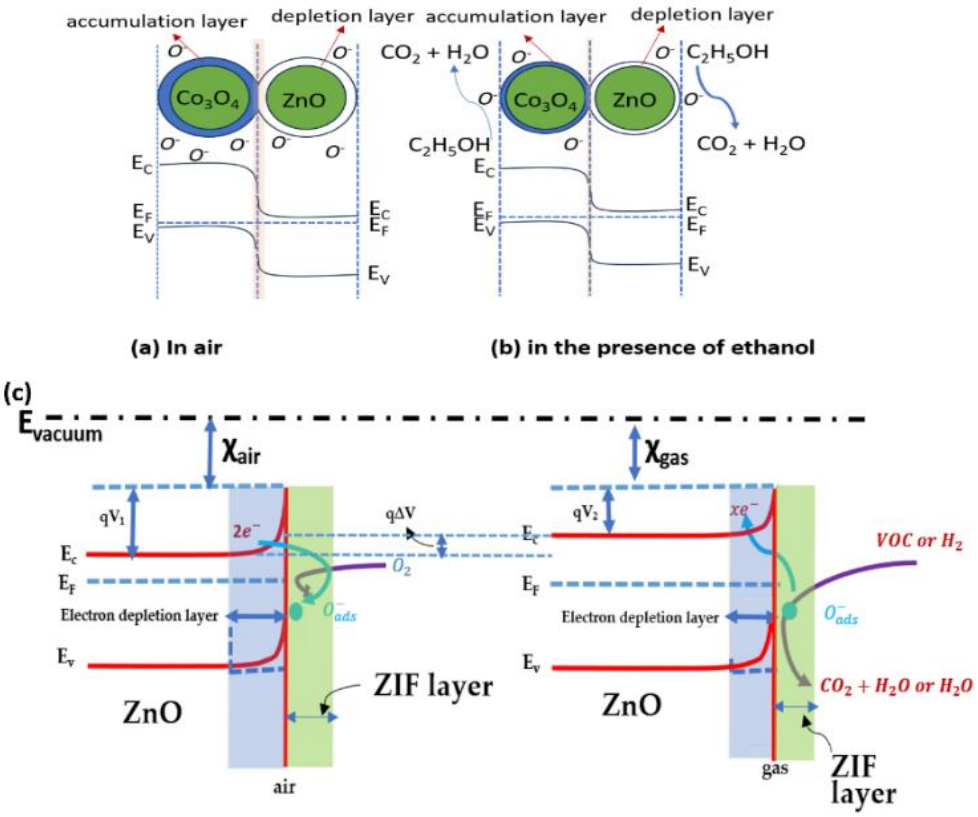

Fig. 13. Proposed gas sensing mechanism of Co_3O_4-ZnO heterostructures (a) in air and (b) in ethanol. (c) Schematic of the gas sensing mechanism of ZIF-coated ZnO, illustrating energy band diagrams upon exposure to reducing gases (VOCs and H_2).

Each chapter of the thesis ends with the research conclusions of research and a summary of the main results obtained. The final conclusions and recommendations express the main results published in journals, which justify the practical applications of the research on the developed hybrid structures.

GENERAL CONCLUSIONS AND RECOMMENDATIONS

The proposed research aimed to develop hybrid structures, namely nanostructured and microstructured Metal-Organic Framework (MOF)-metal oxide systems, based on ZIF/CuO:Al or ZIF/ZnO for the enhancement of functionality. They were accompanied by an advanced characterization for their structural and chemical analysis, in order to correlate the physicochemical properties with sensing mechanisms under adverse environmental conditions. Through the synergistic integration of ZIF metal-organic networks with doped metal oxides, hybrid sensors with high thermal stability and superior performance of selective detection of hydrogen and VOCs have been developed, demonstrating a remarkable potential for environmental monitoring under extreme humidity conditions. Thus, based on the obtained results, the following general **conclusions** can be formulated:

1. A fundamental understanding of the thermal degradation and phase transition mechanisms of the investigated ZIF-based MOFs was achieved by determining their thermal stability ranges, confirming stable operations of ZIF-67, ZIF-7, ZIF-71, and ZIF-8 up to 250 ℃, 375 ℃, 350 ℃, and 350 ℃, respectively [5] [6] [49].
2. The ZIF-8/CuO:Al-based hybrid sensor exhibited well defined structural integrity, high surface area, and stable morphology, with strong confirmation from XRD, SEM, XPS, Raman, and BET analysis. Thermal stability up to 380 ℃ and selective gas sensing performance, particularly for hydrogen and n-butanol, highlight their application potential [5].
3. The ZIF-71/CuO:Al-based hybrid sensor demonstrated a stable monoclinic CuO structure with uniform ZIF-71 deposition, as confirmed by XRD, SEM, XPS, and Raman analysis. The films exhibited nanoscale crystallite size (approx. 57 nm) with larger dimensions (500-700 nm), reflecting coherent growth and surface uniformity [6].
4. ZIFs/ZnO-based study confirmed preferential crystallographic orientations and nanoscale crystallite sizes of all ZIFs (ZIF-67, ZIF-7, ZIF-71, and ZIF-8), with *in-situ* temperature dependent XRD and TGA revealing thermal stability and phase transformations into corresponding oxides. Raman spectroscopy provided detailed vibrational insights, while Cd doping in ZnO induced lattice stress evidenced by Raman peak shifts. Sequential gas-sensing demonstrated selective responses toward alcohols and hydrogen gas, recommending further optimization of doping levels and film architecture for enhanced sensitivity and long-term stability [5] [6] [49].
5. The ZIF-8/CuO:Al-based hybrid sensor exhibited appreciable sensitivity (75%) for 100 ppm hydrogen gas even at a high relative humidity of 81%, enabling its application under adverse conditions. Furthermore, a very low detection limit of 402 ppb was achieved, which is advantageous for various applications, including the detection of very small amount of hydrogen leaks [5,7].
6. The ZIF-8/CuO:Al-based hybrid sensor exhibited appreciable selectivity to hydrogen (>4 times) over other tested analytes such as acetone, 2-propanol, n-butanol, and ethanol at higher temperature (350 ℃) [5,7].
7. ZIF-71/CuO:Al-based hybrid sensor exhibited the selectivity for n-butanol at 200 ℃, which was approximately four times higher than hydrogen gas and about five times higher than acetone during the initial measurements [6].

8. Dual gas sensing (n-butanol and hydrogen) at different operating temperatures (200 ℃ and 250 ℃) exhibited by ZIF-71/CuO:Al can be attributed to the synergistic effect of ZIF-71 and CuO:Al. At lower temperatures (200 ℃), n-butanol selectivity over other tested analytes was observed due to the high polarizability of n-butanol as compared to acetone, it affects the strength of interaction of tested analyte with the ZIF-71 framework. At higher temperatures, hydrogen can easily diffuse through pores and shows higher selectivity at 250 ℃. Further optimization of coating thickness, and device-label testing are recommended to enhance practical sensing performance [6].

Based on the obtained general conclusions, following **recommendations** can be formulated:

1. In order to prevent thermal degradation and phase transitions in ZIF-based MOFs and MOF-metal oxide hybrid structures, operation must be maintained below their respective thermal stability limits: 250 ℃ (ZIF-67), 375 ℃ (ZIF-7), 350 ℃ (ZIF-7), and 350 ℃ (ZIF-8).
2. It is recommended to use simple and cost-effective techniques, such as SCS and microdrop-casting to obtain hybrid structures of ZIF/ZnO or ZIF/CuO.
3. It is recommended to comprehensively characterize material and other physicochemical properties of ZIF-based hybrid structures for their employment in adverse environmental conditions. Thermal test and sorption tests of ZIF-8 particles exhibited its thermal stability up to 380 ℃ and microporous structure, which is advantageous for sensing applications. XPS analysis revealed an intactness of ZIF-8 layer on CuO:Al film, which confirms a successful development of hybrid structures.
4. Hydrophobic nature and thermal stability of ZIF-8 retains its structural framework in adverse environmental conditions. ZIF-8/CuO:Al-based hybrid sensor exhibited appreciable sensitivity (75%) toward 100 ppm hydrogen even at a relative humidity of 81% at 350 ℃. This configuration of hybrid sensor exhibited >4 times hydrogen selectivity compared to other tested analytes, including VOCs (ethanol, acetone, 2-propanol, and n-butanol).
5. It is recommended that uniformly complete coverage of ZIF-71 or ZIF-8 particles on ZnO or CuO enables the employment of hybrid structures in sensing applications. ZIF-71/CuO:Al-based hybrid sensor exhibited four-times higher sensitivity for n-butanol compared to hydrogen and five-times compared to acetone at 200 ℃. At higher temperature (250 ℃), hydrogen selectivity was observed for ZIF-71/CuO:Al-based hybrid sensor.
6. It is recommended to tune the selectivity of alcohol series using an appropriate doping (Cd) in ZIF-67/ZnO based hybrid sensors. ZIF-67/ZnO exhibited higher sensitivity for ethanol compared to other alcohols, but in case of ZIF-67/ZnO:Cd hybrid structures, highest sensitivity was observed for n-butanol or 2-propanol at 250 or 300 ℃.

Bibliography

[1] R. NAGPAL, N. ABABII, O. LUPAN, Comprehensive Advances in Gas Sensing: Mechanisms, Material Innovations, and Applications in Environmental and Health Monitoring, Materials Today Electronics (2025) 100192. https://doi.org/https://doi.org/10.1016/j.mtelec.2025.100192.

[2] L.H.T. NGUYEN, A. MIRZAEI, J.Y. KIM, T.B. PHAN, L.D. TRAN, K.C.W. WU, H.W. KIM, S.S. KIM, T.L.H. DOAN, Advancements in MOF-based resistive gas sensors: synthesis methods and applications for toxic gas detection, Nanoscale Horiz. 10 (2025) 1025–1053. https://doi.org/10.1039/d4nh00662c.

[3] Nobel Foundation, Press release of Nobel prize in Chemistry 2025, 2025. https://www.nobelprize.org/prizes/chemistry/2025/press-release/ (accessed February 9, 2026).

[4] E. GALLEGO, J.F. PERALES, J.M. CALAF, Continuous monitoring of volatile organic compounds through sensorization. Automatic sampling during pollution/odour/nuisance episodic events, Atmos. Environ. 299 (2023) 119657. https://doi.org/https://doi.org/10.1016/j.atmosenv.2023.119657.

[5] R. Nagpal, M. Sugihara, N. Magariu, T. Tjardts, N. Meling-Lizarde, T. Strunskus, T. Ameri, R. Ameloot, R. Adelung, O. Lupan, Humidity-tolerant selective sensing of hydrogen and n-butanol using ZIF-8 coated CuO:Al film, Mater. Chem. Front. 9 (2025) 3425–3442. https://doi.org/10.1039/D5QM00565E.

[6] R. NAGPAL, M. SUGIHARA, C. LUPAN, T. TJARDTS, N. MELING-LIZARDE, T. STRUNSKUS, H. QIU, R. ADELUNG, R. AMELOOT, O. LUPAN, ZIF-71-Coated CuO:Al with Enhanced Gas-Sensing Performance for n-Butanol and Hydrogen, ACS Appl. Electron. Mater. 7 (2025) 10198–10215. https://doi.org/10.1021/acsaelm.5c01659.

[7] O. LUPAN, R. NAGPAL, D. LITRA, M. BRINZA, M. SUGIHARA, R. AMELOOT, S. RAILEAN, T. AMERI, R. ADELUNG, S. SCHRÖDER, F. FAUPEL, Hybrid Nanomaterials for Biomedical Sensors, in: V. Sontea, I. Tiginyanu, S. Railean (Eds.), 7th International Conference on Nanotechnologies and Biomedical Engineering, Springer Nature Switzerland, Cham, 2025: pp. 162–176.

[8] R. NAGPAL, C. LUPAN, A. BÎRNAZ, A. SEREACOV, E. GREVE, M. GRONENBERG, L. SIEBERT, R. ADELUNG, O. LUPAN, Multifunctional Three-in-One Sensor on t-ZnO for Ultraviolet and VOC Sensing for Bioengineering Applications, Biosensors (Basel). 14 (2024) 293. https://doi.org/10.3390/bios14060293.

[9] B. CHAKRABORTY, D. LITRA, A.K. MISHRA, C. LUPAN, R. NAGPAL, S. MISHRA, H. QIU, S. RAILEAN, O. LUPAN, N.H. DE LEEUW, R. ADELUNG, L. SIEBERT, Ultra-selective hydrogen sensors based on CuO - ZnO hetero-structures grown by surface conversion, J. Alloys Compd. 1002 (2024) 175385. https://doi.org/https://doi.org/10.1016/j.jallcom.2024.175385.

[10] M. ATTWA, A. SAID, M. ELGAMAL, Y. EL-SHAER, S. ELBASUNEY, Bespoke Energetic Zeolite Imidazolate Frameworks-8 (ZIF-8)/Ammonium Perchlorate Nanocomposite: A Novel Reactive Catalyzed High Energy Dense Material with Superior Decomposition Kinetics, J. Inorg. Organomet. Polym. Mater. 34 (2024) 387–400. https://doi.org/10.1007/s10904-023-02834-2.

[11] L. MISHRA, V.K. DWIVEDI, H.K. DARA, V.K. CHAKRADHARY, S. ITHINENI, A.G. PRABHUDESSAI, S. NEHAR, Core/Shell-Like Magnetic Structure and Optical Properties in CuO Nanoparticles Synthesized by Green Route, ACS Sustainable Resource Management 1 (2024) 2472–2481. https://doi.org/10.1021/acssusresmgt.4c00325.

[12] B. OLANIYAN, B. SAHA, Comparison of Catalytic Activity of ZIF-8 and Zr/ZIF-8 for Greener Synthesis of Chloromethyl Ethylene Carbonate by CO2 Utilization, Energies (Basel). 13 (2020). https://doi.org/10.3390/en13030521.

[13] J. LIU, Z. GAO, Y. HUANG, Y. SONG, Structural changes and CO2 adsorption performance in Zn2(BDC)2DABCO metal-organic framework under high-pressure and high-temperature conditions, Can. J. Chem. 0 (n.d.) null. https://doi.org/10.1139/cjc-2024-0166.

[14] J. LI, H. CHANG, Y. LI, Q. LI, K. SHEN, H. YI, J. ZHANG, Synthesis and adsorption performance of La@ZIF-8 composite metal–organic frameworks, RSC Adv. 10 (2020) 3380–3390. https://doi.org/10.1039/C9RA10548D.

[15] J. NARIMBI, S. BALAKRISHNAN, T.S. PEROVA, G. DEE, G.F. SWIEGERS, Y.K. GUN'KO, XRD and Spectroscopic Investigations of ZIF—Microchannel Glass Plates Composites, Materials 16 (2023). https://doi.org/10.3390/ma16062410.

[16] A. DEACON, L. BRIQUET, M. MALANKOWSKA, F. MASSINGBERD-MUNDY, S. RUDIĆ, T. L. HYDE, H. CAVAYE, J. CORONAS, S. POULSTON, T. JOHNSON, Understanding the ZIF-L to ZIF-8 transformation from fundamentals to fully costed kilogram-scale production, Commun. Chem. 5 (2022). https://doi.org/10.1038/s42004-021-00613-z.

[17] G. MANI, A. V KUMAR, S. MATHEW, ZIF-8 derived ZnO: a facile catalyst for ammonium perchlorate thermal decomposition††Electronic supplementary information (ESI) available. See DOI: https://doi.org/10.1039/d3su00256j, RSC Sustainability 1 (2023) 2081–2091. https://doi.org/https://doi.org/10.1039/d3su00256j.

[18] J. QIU, X. XU, B. LIU, Y. GUO, H. WANG, L. YU, Y. JIANG, C. HUANG, B. FAN, Z. ZENG, L. LI, Size-Controllable Synthesis of ZIF-8 and Derived Nitrogen-Rich Porous Carbon for CO_2 and VOCs Adsorption, ChemistrySelect 7 (2022) e202203273. https://doi.org/https://doi.org/10.1002/slct.202203273.

[19] R. NAGPAL, C. LUPAN, A. BUZDUGAN, V. GHENEA, O. LUPAN, Effect of Pd functionalization on optical and hydrogen sensing properties of ZnO: Eu films, Optik (Stuttg). (2025) 172247. https://doi.org/https://doi.org/10.1016/j.ijleo.2025.172247.

[20] F. DE SOUZA LUCAS, H. PENG, S. JOHNSTON, P.C. DIPPO, S. LANY, L.H. MASCARO, A. ZAKUTAYEV, Characterization of defects in copper antimony disulfide, J. Mater. Chem. A 5 (2017) 21986–21993. https://doi.org/10.1039/C7TA07012H.

[21] A.I.A. SOLIMAN, A.M.A. ABDEL-WAHAB, H.N. ABDELHAMID, Hierarchical porous zeolitic imidazolate frameworks (ZIF-8) and ZnO@N-doped carbon for selective adsorption and photocatalytic degradation of organic pollutants, RSC Adv. 12 (2022) 7075–7084. https://doi.org/10.1039/d2ra00503d.

[22] P. SHANKAR, J.B.B. RAYAPPAN, Room temperature ethanol sensing properties of ZnO nanorods prepared using an electrospinning technique, J. Mater. Chem. C 5 (2017) 10869–10880. https://doi.org/10.1039/C7TC03771F.

[23] C. GAO, J. WU, Q. SHI, H. YING, J. DONG, Adsorption breakthrough behavior of 1-butanol from an ABE model solution with high-silica zeolite: Comparison with zeolitic imidazolate frameworks (ZIF-8), Microporous and Mesoporous Materials 243 (2017) 119–129. https://doi.org/https://doi.org/10.1016/j.micromeso.2017.02.009.

[24] O. LUPAN, V. CRETU, V. POSTICA, N. ABABII, O. POLONSKYI, V. KAIDAS, F. SCHÜTT, Y.K. MISHRA, E. MONAICO, I. TIGINYANU, V. SONTEA, T. STRUNSKUS, F. FAUPEL, R. ADELUNG,

Enhanced ethanol vapour sensing performances of copper oxide nanocrystals with mixed phases, Sens. Actuators B Chem. 224 (2016) 434–448. https://doi.org/https://doi.org/10.1016/j.snb.2015.10.042.

[25] X. DONG, Y.S. LIN, Synthesis of an organophilic ZIF-71 membrane for pervaporation solvent separation, Chem. Commun. 49 (2013) 1196–1198. https://doi.org/10.1039/C2CC38512K.

[26] A.F. MÖSLEIN, J.-C. TAN, Vibrational Modes and Terahertz Phenomena of the Large-Cage Zeolitic Imidazolate Framework-71, J. Phys. Chem. Lett. 13 (2022) 2838–2844. https://doi.org/10.1021/acs.jpclett.2c00081.

[27] J. ETHIRAJ, F. BONINO, C. LAMBERTI, S. BORDIGA, H_2S interaction with HKUST-1 and ZIF-8 MOFs: A multitechnique study, Microporous and Mesoporous Materials 207 (2015) 90–94. https://doi.org/https://doi.org/10.1016/j.micromeso.2014.12.034.

[28] J. YE, J.-C. TAN, J. YE, J. TAN, High-Performance Triboelectric Nanogenerators Incorporating Chlorinated Zeolitic Imidazolate Frameworks with Topologically Tunable Dielectric and Surface Adhesion Properties, Nano Energy (2023). https://doi.org/https://doi.org/10.1016/j.nanoen.2023.108687.

[29] Y. DENG, A.D. HANDOKO, Y. DU, S. XI, B.S. YEO, In Situ Raman Spectroscopy of Copper and Copper Oxide Surfaces during Electrochemical Oxygen Evolution Reaction: Identification of CuIII Oxides as Catalytically Active Species, ACS Catal. 6 (2016) 2473–2481. https://doi.org/10.1021/acscatal.6b00205.

[30] Y. ZHANG, M. GUTIÉRREZ, A.K. CHAUDHARI, J.-C. TAN, Dye-Encapsulated Zeolitic Imidazolate Framework (ZIF-71) for Fluorochromic Sensing of Pressure, Temperature, and Volatile Solvents, ACS Appl. Mater. Interfaces 12 (2020) 37477–37488. https://doi.org/10.1021/acsami.0c10257.

[31] G. ORTIZ, H. NOUALI, C. MARICHAL, G. CHAPLAIS, J. PATARIN, Energetic Performances of "ZIF-71–Aqueous Solution" Systems: A Perfect Shock-Absorber with Water, The Journal of Physical Chemistry C 118 (2014) 21316–21322. https://doi.org/10.1021/jp505484x.

[32] J. FARRANDO-PEREZ, A. MISSYUL, A. MARTÍN-CALVO, C. ABREU-JAUREGUI, V. RAMÍREZ-CEREZO, L. DAEMEN, Y.Q. CHENG, A.J. RAMIREZ-CUESTA, S. CALERO, C. CARRILLO-CARRIÓN, J. SILVESTRE-ALBERO, Molecular recognition-induced structural flexibility in ZIF-71, J. Mater. Chem. A Mater. (2024). https://doi.org/10.1039/d4ta03813d.

[33] D.O. SCANLON, B.J. MORGAN, G.W. WATSON, A. WALSH, Acceptor Levels in p-Type Cu_2O Rationalizing Theory and Experiment, Phys. Rev. Lett. 103 (2009) 96405. https://doi.org/10.1103/PhysRevLett.103.096405.

[34] H. RAEBIGER, S. LANY, A. ZUNGER, Origins of the p-type nature and cation deficiency in Cu_2O and related materials, Phys. Rev. B 76 (2007) 45209. https://doi.org/10.1103/PhysRevB.76.045209.

[35] L. MALEPE, T.D. NDINTEH, P. NDUNGU, M.A. MAMO, A humidity tolerance and room temperature carbon soot@ZIF-71 sensor for toluene vapour detection, Mater. Res. Bull. 181 (2025) 113076. https://doi.org/https://doi.org/10.1016/j.materresbull.2024.113076.

[36] W. LI, T. MA, P. TANG, Y. LUO, H. ZHANG, J. ZHAO, R. AMELOOT, M. TU, Nanoscale Resist-Free Patterning of Halogenated Zeolitic Imidazolate Frameworks by Extreme UV Lithography, Advanced Science 12 (2025) 2415804. https://doi.org/https://doi.org/10.1002/advs.202415804.

[37] Z. SHAO, L. DING, W. ZHU, C. FAN, K. DI, R. YUAN, K. WANG, Highly selective detection and removal of mercury ions in the aquatic environment based on magnetic ZIF-71 multifunctional composites with sufficient chlorine functional groups, Science of The Total Environment 921 (2024) 171085. https://doi.org/https://doi.org/10.1016/j.scitotenv.2024.171085.

[38] S. BHATTACHARYYA, K.C. JAYACHANDRABABU, Y. CHIANG, D.S. SHOLL, S. NAIR, Butanol Separation from Humid CO_2-Containing Multicomponent Vapor Mixtures by Zeolitic Imidazolate Frameworks, ACS Sustain. Chem. Eng. 5 (2017) 9467–9476. https://doi.org/10.1021/acssuschemeng.7b02604.

[39] X. FENG, M.A. CARREON, Kinetics of transformation on ZIF-67 crystals, J. Cryst. Growth 418 (2015) 158–162. https://doi.org/https://doi.org/10.1016/j.jcrysgro.2015.02.064.

[40] B.N. JOSHI, J.-G. LEE, S. AN, D.-Y. KIM, J.S. LEE, Y.K. HWANG, J.-S. CHANG, S.S. AL-DEYAB, J.-C. TAN, S.S. YOON, Tuning crystalline structure of zeolitic metal–organic frameworks by supersonic spraying of precursor nanoparticle suspensions, Mater. Des. 114 (2017) 416–423. https://doi.org/https://doi.org/10.1016/j.matdes.2016.11.001.

[41] R. BANERJEE, A. PHAN, B. WANG, C. KNOBLER, H. FURUKAWA, M. O'KEEFFE, O.M. YAGHI, High-throughput synthesis of zeolitic imidazolate frameworks and application to CO2 capture, Science (1979). 319 (2008) 939–943.

[42] M. THI THANH, T. VINH THIEN, V. THI THANH CHAU, P. DINH DU, N. PHI HUNG, D. QUANG KHIEU, Synthesis of Iron Doped Zeolite Imidazolate Framework-8 and Its Remazol Deep Black RGB Dye Adsorption Ability, J. Chem. 2017 (2017) 5045973. https://doi.org/https://doi.org/10.1155/2017/5045973.

[43] O. LUPAN, T. PAUPORTÉ, T. LE BAHERS, I. CIOFINI, B. VIANA, High Aspect Ratio Ternary $Zn_{1-x}Cd_xO$ Nanowires by Electrodeposition for Light-Emitting Diode Applications, The Journal of Physical Chemistry C 115 (2011) 14548–14558. https://doi.org/10.1021/jp202608e.

[44] G.-R. LI, W.-X. ZHAO, Q. BU, Y.-X. TONG, A novel electrochemical deposition route for the preparation of $Zn_{1-x}Cd_xO$ nanorods with controllable optical properties, Electrochem. Commun. 11 (2009) 282–285. https://doi.org/https://doi.org/10.1016/j.elecom.2008.11.024.

[45] Y. SUN, Y. LI, J.-C. TAN, Liquid Intrusion into Zeolitic Imidazolate Framework-7 Nanocrystals: Exposing the Roles of Phase Transition and Gate Opening to Enable Energy Absorption Applications, ACS Appl. Mater. Interfaces 10 (2018) 41831–41838. https://doi.org/10.1021/acsami.8b16527.

[46] X. YANG, S. JIANG, Z. ZHANG, B. LI, M. XU, The preparation of ZIF-67 and its synergistic effect on fire performance of intumescent flame retardant polypropylene, J. Therm. Anal. Calorim. 148 (2023) 9547–9560. https://doi.org/10.1007/s10973-023-12316-9.

[47] M. MARTÍNEZ-SALAZAR, N. TIEMPOS FLORES, A. OBREGÓN-ZÚÑIGA, O.I. ARILLO-FLORES, N.E. DÁVILA-GUZMÁN, D.J. MICHAELIS, J. RAZIEL ÁLVAREZ, E. HERNÁNDEZ-FERNÁNDEZ, Dye Removal Utilizing ZIF-71 and Hydrophobic ZIF-71(ClBr): Kinetic and Equilibrium Studies, ACS Omega 10 (2025) 43404–43414. https://doi.org/10.1021/acsomega.4c09336.

[48] T.P. MOKOENA, H.C. SWART, K.T. HILLIE, Z.P. TSHABALALA, M. JOZELA, J. TSHILONGO, D.E. MOTAUNG, Enhanced propanol gas sensing performance of p-type NiO gas sensor induced by

exceptionally large surface area and crystallinity, Appl. Surf. Sci. 571 (2022) 151121. https://doi.org/https://doi.org/10.1016/j.apsusc.2021.151121.

[49] RAJAT, Nagpal, SUGIHARA, M., LUPAN, C., MAGARIU, N., TJARDTS, T., MELING-LIZARDE, N., STRUNSKUS, T., JETTER. J., QIU, H., CHAKRABORTY, B., AMERI, T., QUANDT, E., ADELUNG, R., AMELOOT, R., LUPAN, O. In-situ temperature-dependent properties of metal-organic frameworks ZIF-coated ZnO hybrid structures: structural and advanced spectroscopic insights, revised/accepted, ACS Omega, March, 2026.

LIST OF THE AUTHOR'S PUBLICATIONS ON THE SUBJECT OF THE Ph.D. THESIS

Articles in international journals listed in ISI and SCOPUS:

1. **RAJAT Nagpal**, ABABII, N., LUPAN, O., Comprehensive Advances in Gas Sensing: Mechanisms, Material Innovations, and Applications in Environmental and Health Monitoring, *Material Today Electronics* 2026, 15, 100192, ISSN 2772-9494, *Accepted 10 December* 2025, https://doi.org/10.1016/j.mtelec.2025.100192 **(Impact Factor: 7.4)**
2. **RAJAT, Nagpal**, SUGIHARA, M., MAGARIU, N., TJARDTS, T., MELING-LIZARDE, N., STRUNSKUS, T., AMERI, T., AMELOOT, R., ADELUNG, R., LUPAN, O. Humidity- tolerant selective sensing of hydrogen, and n-butanol using ZIF-8 coated CuO:Al films, *Materials Chemistry Frontiers* 2025, 9, pp. 3425-3442, https://doi.org/10.1039/D5QM00565E (**Impact Factor: 6.4)**
3. **RAJAT, Nagpal**, SUGIHARA, M., LUPAN, C., TJARDTS, T., MELING-LIZARDE, N., STRUNSKUS, T., QIU, H., ADELUNG, R., AMELOOT, R., LUPAN, O. ZIF-71 coated CuO:Al with enhanced gas sensing performance for n-butanol and hydrogen, *Appl Elec Mater* 2025, 7, pp. 10198-10215, https://doi.org/10.1021/acsaelm.5c01659 (**Impact Factor: 4.7)**
4. **RAJAT, Nagpal**, LUPAN, C., BUZDUGAN, A., GHENEA, V., LUPAN, O. Effect of Pd functionalization on optical and hydrogen sensing properties of ZnO: Eu films, *Optik* 2025, 325, 172247, https://doi.org/10.1016/j.ijleo.2025.172247 **(Impact Factor: 3.1)**
5. **RAJAT, Nagpal**, LUPAN, C., BÎRNAZ, A., SEREACOV, A., GREVE, E., GRONENBERG, M., SIEBERT, L.; ADELUNG, R.; LUPAN, O. Multifunctional Three-in-One Sensor on t-ZnO for Ultraviolet and VOC Sensing for Bioengineering Applications, *Biosensors* 2024, 14, pp. 293, https://doi.org/10.3390/bios14060293 **(Impact Factor: 5.6)**
6. **RAJAT, Nagpal**, SUGIHARA, M., LUPAN, C., MAGARIU, N., TJARDTS, T., MELING-LIZARDE, N., STRUNSKUS, T., JETTER. J., QIU, H., CHAKRABORTY, B., AMERI, T., QUANDT, E., ADELUNG, R., AMELOOT, R., LUPAN, O. In-situ temperature-dependent XRD and advanced spectroscopic insights and defect-mediated properties in ZIF-coated ZnO hybrid structures, submitted in *ACS Applied Nano Materials*, under review (**Impact Factor: 5.5)**

In journals from the National Register of specialized journals, indicating the category:

7. **RAJAT, Nagpal,** CHIRIAC, M., SEREACOV, A., BIRNAZ, A., ABABII, N., LUPAN, C., BUZDUGAN, A., SANDU, I., SIEBERT, L., PAUPORTÉ, T., LUPAN, O., ANNEALING EFFECT ON UV DETECTION PROPERTIES OF ZnO:Al STRUCTURES, *Journal of Engineering Science*, Vol. 30 (4) 2023, pp. 45–62, https://doi.org/10.52326/jes.utm.2023.30(4).04, ISSN: 287-3474, B^+

Articles in the proceedings of scientific events included in the Web of Science and SCOPUS databases:

8. **RAJAT, Nagpal,** CHIRIAC, M., SUGIHARA, M., LITRA, D., MAGARIU, N., LUPAN, C., ZINICOVSCHI, V., AMELOOT, R., LUPAN, O. Sensory Properties of CuO/Cu_2O Nanostructures Coated with Zeolitic Imidazolate Frameworks, *E-Health and Bioengineering Conference (EHB)*, IASI, Romania, *IEEE Xplore*, 2024, pp. 1-4, doi: 10.1109/EHB64556.2024.10805729, **ISBN:**979-8-3315-3214-7
9. LUPAN, O., **RAJAT, Nagpal**, LITRA, D., BRINZA, M., SUGIHARA, M., AMELOOT, R., SERGHEI, R., AMERI, T., ADELUNG, R., SCHRODER, S., FAUPEL, F., Hybrid Nanomaterials for Biomedical Sensors, *7th International Conference on Nanotechnologies and Biomedical Engineering*, *2025*, *IFMBE Proceedings,* vol 134. *Springer*, pp. 162-176, Cham. https://doi.org/10.1007/978-3-032-06494-3_18, ISBN: 978-3-032-06494-3
10. **RAJAT, Nagpal,** LUPAN, C., VIANA, B., PAUPORTÉ, T., LUPAN, O., ADELUNG, R., Study on the Optical and Gas Sensing Properties of Eu-Doped ZnO, *IEEE 14th International Conference Nanomaterials: Applications and Properties)* , *IEEE Xplore*, 2024, pp. 1-4, https://doi.org/10.1109/NAP62956.2024.10739686, **ISBN:** 979-8-3503-8012-5

Articles in the proceedings of national conferences scientific events:

11. **RAJAT, Nagpal**, LUPAN, C., SANDU, I., BÎRNAZ**,** A. UV LIGHT DETECTION BASED ON ZnO NETWORKS. *At the conference: Integration through research and innovation*, State University of Moldova, Chisinau, Moldova, November 9-10, 2023, pp. 752-757, Available: https://ibn.idsi.md/vizualizare_articol/201035, ISBN: 978-9975-62-687-3

In the volume of abstracts of international scientific conferences (abroad)

12. **RAJAT, Nagpal**, SIEBERT, L., LUPAN, C., PADUNNAPPATTU, A., POSCHMANN, MIRJAM P.M., STOCK, N., ADELUNG, R., LUPAN, O. Metal Organic Framework based low powered ultraviolet signal detection. Poster presentation: *MOFSIM 2024,* Montpellier, April 10-12, 2024, pp. 90 (Book of Abstracts). Available:https://drive.google.com/file/d/10KpC8RzHq7JqZbHrqf2nRcGnRRZMFmg2/view
13. LUPAN, O., BRINZA, M., LITRA, D., **RAJAT, Nagpal**, SCHRODER, S., SUGIHARA, M., STRUNSKUS, T., AMELOOT, R., AMERI, T., ADELUNG, R., FAUPEL, F., Nanomaterials for Biomedical and Industrial Hybrid Sensors, *IEEE 15th International Conference on "Nanomaterials: Applications & Properties",* Bratislava, Slovakia, Sept. 7-12, 2025, pp. 09nna-10 – 09nna-11 (Book of Abstracts). Available: https://ieeenap.org/data/Book_of_Abstracts_2025.pdf

Patents issued by the State Agency for Intellectual Property:

14. RAJAT, Nagpal, SUGIHARA, M., MAGARIU, N., TROFIM V., LUPAN, C., AMELOOT, R., Process for manufacturing hydrogen sensor based on CuO:Al-ZIF-8 nanostructures, Patent app., **entr. no.** 7587 date 23.10.2025, AGEPI

ABSTRACT

In the Ph.D. thesis entitled „**Porous Networks of Nanostructured Hybrid Materials**", submitted by **Rajat,** for conferring the scientific joint doctoral degree in physical sciences at Technical University of Moldova (UTM), in the speciality 134.03 „Physics of nanosystems and nanotechnologies", and in engineering at Kiel University, Germany.

Structure of the thesis: The thesis was carried out jointly at the UTM, Department of Microelectronics and Biomedical Engineering, Center for Nanotechnology and Nanosensors and Kiel University, Faculty of Engineering, Chair for Functional Nanomaterials, Germany. The thesis is written in English language and consists of an introduction, five chapters, general conclusions and recommendations, bibliography with 273 references, 104 pages of basic text, 40 figures, 7 tables, and 37 equations. The research results obtained were published in 25 scientific publications, 14 of which are directly related to the topic of the thesis, including one patent application; six peer-reviewed articles in international journals indexed in the ISI, WoS, and SCOPUS databases. All peer-reviewed articles were published open-access in journals with an impact factor greater than 3. One article in JES (Journal of Engineering Sciences) and six works were presented and published at National and International Conferences after review.

Keywords: MOFs, ZIFs, ZnO, CuO, synergistic, molecular sieving effect, hybrid materials, MOF/MO, sensor.

Research purpose: This PhD thesis aims to develop hybrid materials/systems based on metal-organic frameworks/metal oxide (MOF/MO) for improved functionality, advanced characterization for detailed investigation of their physicochemical properties and establishing their correlation with sensing performance. The main objectives include evaluating the performance of the developed MOF/MO hybrid systems and sensors for selective detection of target analytes (hydrogen and volatile organic compounds) under adverse environmental conditions, elucidating the corresponding detection mechanism and enabling differentiation of analytes.

Objectives: An extensive investigation of physicochemical properties of the ZIF/ZnO and ZIF/CuO based MOF/MO hybrid structures and their employment for gas sensing applications based on metal-organic framework (MOF)-metal oxide (MOF/MO) systems: (i) ZIF-71/CuO:Al, for the detection of hydrogen and n-butanol at different operating temperatures; (ii) ZIF-8/CuO:Al hybrid structures for hydrogen and VOCs sensing under adverse environmental conditions; (iii) development of multi-sensors arrays for complex analyte differentiation using ZIFs/ZnO and ZIFs/Cd-doped ZnO based MOF/MO hybrid structures.

Scientific originality and the novelty of the research: Hybrid structures based on metal-organic framework (MOF)-metal oxide (MOF/MO) systems, namely ZIF/ZnO structures, were developed using a simple and cost-effective approach. A detailed investigation of physicochemical properties of the ZIFs/ZnO and ZIFs/CuO-based hybrid materials and the establishment of a methodology to correlate structure-property-performance relationship for the selective detection of tested analytes, including volatile compounds VOCs and hydrogen gas in adverse environmental conditions is novel which makes it interesting for the scientific community. A methodology combining *in-situ* analysis at different temperatures with sequential detection for comprehensive gas differentiation using multiple sensors was established. The ZIF-8/CuO:Al-based hybrid structures exhibited appreciable gas response (75%) to 100 ppm hydrogen, even at a relative humidity of RH 81%, enabling their applications under adverse humid conditions for extended periods of investigations. The developed ZIF-71/CuO:Al hybrid sensor exhibited dual gas sensing for n-butanol and hydrogen at different operating temperatures of 200 °C and 250 °C, respectively.

The scientific problem addressed: The research work established structure-property-performance correlations of hybrid structures based on metal-organic framework (MOF)-metal oxide (MOF/MO) systems−for example, ZIF-n (n = 67, 7, 71, 8) combined with metal oxides such as ZnO:Cd and CuO:Al. The synergistic effect of different metal oxides with MOFs on their gas sensing performance to VOCs and hydrogen under adverse conditions was identified. Highly sensitive and selective hydrogen gas detection, even in high-humidity conditions and at low detection limits, opens up new areas of applicability.

The theoretical significance and applications of the work: The theoretical significance lies in establishing structure-property-performance relationships by determining the thermal stability ranges and oxidative transformation pathways of metal-organic frameworks ZIF-n (n = 67, 7, 71, 8) and metal oxides (Co_3O_4/ZnO) through *in-situ* structural analysis at different temperatures, thus defining their fundamental operational limits and mechanistic contributions in gas sensing. Establishing a critical understanding of the radiolytic stability of halogenated MOFs by identifying X-ray-induced degradation in ZIF-71, thus elucidating how specific functional groups dictate structural integrity under ionizing radiation and defining the thresholds necessary for non-destructive characterization. The ZIF-8/CuO:Al-based hybrid structures exhibited selective detection of hydrogen compared to other tested analytes and a low detection limit of ~402 ppb was achieved, which is advantageous for various applications, including the detection of very small amounts of hydrogen gas leaks. ZIF-71/CuO:Al-based hybrid structures exhibited dual gas sensing performance for n-butanol and hydrogen at 200 °C and 250 °C, respectively, where n-butanol sensing response at 200 °C is four times higher than response to hydrogen gas. ZIF-67/ZnO hybrid sensor exhibited ethanol selectivity at 250 °C, where as selectivity to hydrogen was observed for other three hybrid structures (ZIF-7/ZnO, ZIF-71/ZnO, and ZIF-8/ZnO). The practical applications of the presented work in wearable device applications for the effective sensing performance of hydrogen and different VOCs in indoor and outdoor environment and possible radiolytic detection.

Implementation of scientific results: The obtained scientific results were partially implemented within the DMIB-FCIM at the UTM, as well as one patent application.

ADNOTARE

la teza de doctorat întitulată „**Rețele Poroase de Materiale Hibride Nanostructurate**“, prezentată de **Rajat**, pentru conferirea titlului științific de doctor în științe fizice la Universitatea Tehnică a Moldovei (UTM), specialitatea 134.03 „Fizica nanosistemelor și nanotehnologiilor“ și în inginerie la Universitatea din Kiel (în cotutelă).

Structura tezei: Teza a fost realizată în comun la UTM, Centrul de Nanotehnologii și Nanosenzori, Departamentul Microelectronică și Inginerie Biomedicală și Universitatea din Kiel, Facultatea de Inginerie, Catedra Nanomateriale Funcționale, Germania (în cotutelă). Teza este scrisă în limba engleză și constă dintr-o introducere, cinci capitole, concluzii generale și recomandări, o bibliografie cu 273 de referințe, 104 pagini de text de bază, 40 de figuri, 7 tabele și 37 de ecuații. Rezultatele obținute au fost diseminate în 25 lucrări științifice, dintre care 14 sunt direct corelate cu tema tezei, incluzând: o cerere de brevet de invenție; 6 articole recenzate în reviste internaționale indexate în bazele de date ISI, Web of Science și Scopus. Toate articolele recenzate au fost publicate Open Access în reviste cu un factor de impact mai mare de 3, iar un articol în revista JES și 6 lucrări prezentate și publicate la conferințe.

Cuvinte-cheie: MOF, ZIF, ZnO, CuO, sinergic, efect de cernere moleculară, materiale hibride, MOF/MO, senzor.

Scopul cercetării: Teză de doctorat își propune să dezvolte sisteme hibride de tip oxid metalic-rețea metalo-organică (MOF/MO) pentru o caracterizare avansată a proprietăților fizico-chimice și stabilirea corelației acestora cu performanța și funcționalitate îmbunătățită de detecție a gazelor (compușilor organici volatili (COV) și hidrogen). Evaluarea fizico-chimică avansată a sistemelor hibride oxid metalic-rețea metal-organică și a senzorilor pentru detectarea selectivă a analiților (hidrogen și COV) în diverse condiții de mediu, elucidarea mecanismului de detectare corespunzător pe baza răspunsurilor utilizând senzori multipli din MOF/MO_x.

Obiective: O investigație extinsă a proprietăților fizico-chimice ale structurilor hibride pe bază de ZIF/ZnO sau ZIF/CuO și utilizarea acestora în aplicații de senzor pe baza sistemelor de oxid metalic-rețele metalo-organice (MOF/MO): (i) ZIF-71/CuO:Al, pentru detecția hidrogenului și a n-butanolului la diferite temperaturi de operare; (ii) structuri hibride de tip ZIF-8/CuO:Al pentru detectarea hidrogenului și a COV în diverse medii; (iii) dezvoltarea matricelor multisenzori utilizând structuri hibride MOF/MO, în particular ZIFs/ZnO și ZIFs/ZnO:Cd.

Originalitate științifică și noutatea cercetării: Structurile hibride MOF/MO bazate pe rețele metalo-organice (MOF)-oxid metalic, și anume heterostructuri ZIF/ZnO. O investigație detaliată a proprietăților fizico-chimice ale materialelor hibride pe bază de ZIF/ZnO și ZIF/CuO și stabilirea unei metodologii pentru corelarea relației structură-proprietate-performanță pentru detectarea selectivă a compușilor organici volatili COV și hidrogen, reprezintă o noutate pentru comunitatea științifică. A fost stabilită o metodologie care combină analiza *in-situ* cu detectarea secvențială pentru diferențierea completă a analiților de test utilizând senzori multipli pe bază de MOF/MO. Structurile hibride pe bază de ZIF-8/CuO:Al au prezentat un răspuns înalt (75%) față de 100 ppm hidrogen chiar și la o umiditate relativă ridicată de 81%, permițând aplicațiile acestora în condiții de umiditate pentru perioade lungi de timp. Senzorul hibrid pe bază de ZIF-71/CuO:Al dezvoltat a demonstrat o detecție dual a gazelor (n-butanol și hidrogen) la temperaturi de operare diferite, 200°C și 250°C, respectiv.

Problema științifică abordată: Lucrarea a stabilit corelații structură-proprietăți-performanță ale structurilor hibride bazate pe rețele MOF/MO. A fost identificat efectul sinergic al diferiților oxizi metalici cu MOF asupra performanței lor de detecție a COV și a H_2. Detectarea H_2 cu răspuns și selectivitate ridicată, chiar și în condiții de umiditate înaltă și limite de detecție scăzute, deschide noi domenii de aplicabilitate.

Semnificația teoretică și aplicațiile lucrării: Semnificația teoretică rezidă în stabilirea relațiilor structură-proprietate-performanță prin determinarea intervalelor de stabilitate termică și a căilor de transformare oxidativă ale rețelelor metalo-organice de tip ZIF (ZIF-67, ZIF-7, ZIF-71 și ZIF-8) și a oxizilor metalici dopați prin analiză structurală *in-situ*, definind astfel limitele operaționale fundamentale și contribuțiile la mecanismul senzor. Înțelegerea stabilității radiolitice a MOF prin identificarea degradării induse de razele X în ZIF-71, elucidând astfel modul în care grupele funcționale specifice dictează integritatea structurală sub acțiunea radiațiilor ionizante și definind pragurile necesare pentru o caracterizare non-distructivă. Structurile hibride pe bază de ZIF-8/CuO:Al au prezentat o detectare selectivă a H_2 în comparație cu alți analiți testați și s-a atins o limită de detecție de doar ~402 ppb, ceea ce este avantajos pentru diverse aplicații, inclusiv detectarea unor cantități foarte mici de scurgeri incipiente de H_2. Structurile hibride pe bază de ZIF-71/CuO:Al au prezentat performanțe duale de detectare a gazelor pentru n-butanol și H_2 gaz la 200 °C și respectiv 250 °C, unde răspunsul de detectare a n-butanol la 200 °C este de patru ori mai mare decât răspunsul la H_2 gazos. Senzorul hibrid ZIF-67/ZnO a prezentat selectivitate pentru etanol la 250 °C, în timp ce selectivitatea față de H_2 a fost observată pentru alte structuri hibride (ZIF-7/ZnO, ZIF-71/ZnO și ZIF-8/ZnO). Aplicațiile practice pot fi pentru detectare eficientă a H_2 și a diferiților analiți (COV) în medii interioare și exterioare și detecție radiolitică.

Implementarea rezultatelor științifice: Rezultatele științifice obținute au fost implementate parțial în cadrul DMIB-FCIM din cadrul UTM, fiind depusă, de asemenea, o cerere de brevet de invenție.

KURZFASSUNG

In der Dissertation mit dem Titel **„Porous Networks of Nanostructured Hybrid Materials“**, eingereicht von **Rajat** zur Erlangung des gemeinsamen akademischen Grades eines Doktors der Naturwissenschaften an der Technischen Universität Moldau (UTM) im Fachbereich 134.03 „Physik von Nanosystemen und Nanotechnologien“ sowie des Grades eines Doktors der Ingenieurwissenschaften an der Universität zu Kiel.

Struktur der Dissertation: Die Dissertation wurde gemeinsam an der UTM, DMBE, Zentrum für Nanotechnologie und Nanosensoren und der Universität zu Kiel, Technische Fakultät, Lehrstuhl für Funktionale Nanomaterialien. Die Arbeit ist in englischer Sprache verfasst und gliedert sich in eine Einleitung, fünf Kapitel, allgemeine Schlussfolgerungen und Empfehlungen, ein Literaturverzeichnis mit 273 Quellen, 104 Seiten Haupttext, 40 Abbildungen, 7 Tabellen und 37 Gleichungen. Die erzielten Ergebnisse wurden in 25 wissenschaftlichen Publikationen veröffentlicht, von denen 14 einen direkten Bezug zum Thema der Dissertation aufweisen. Dazu gehören: eine Patentanmeldung, 6 begutachtete Artikel (Peer-Review) in internationalen Fachzeitschriften, die in den Datenbanken ISI und Scopus indexiert sind. Sämtliche begutachteten Artikel wurden als Open-Access-Publikationen veröffentlicht. Zudem wurden ein Artikel im JES publiziert und 6 Beiträge auf nationalen sowie internationalen Konferenzen präsentiert.

Schlüsselwörter: MOFs, ZIFs, ZnO, CuO, Synergie, Molekularsiebeffekt, Hybridmaterialien, MOF/MO, der Sensor.

Forschungsziel: Diese Dissertation zielt auf die Entwicklung von Hybridsystemen auf Basis von Metalloxiden und MOFs zur Verbesserung der Funktionalität, die Anwendung fortschrittlicher Charakterisierungsmethoden zur detaillierten Untersuchung ihrer physikalisch-chemischen Eigenschaften sowie die Etablierung ihrer Korrelation mit den Detektionsmechanismen ab. Zu den Hauptzielen gehören die Leistungsbewertung der entwickelten Hybridsysteme und Sensoren zur selektiven Detektion von Zielanalyt-Gasen (Wasserstoff und VOCs) unter widrigen Umweltbedingungen, die Aufklärung der entsprechenden Detektionsmechanismen.

Zielsetzung: Eine umfassende Untersuchung der physikalisch-chemischen Eigenschaften von ZIF/ZnO- oder ZIF/CuO-Hybridstrukturen und deren Einsatz für Sensoranwendungen basierend auf: (i) ZIF-71/CuO:Al zur Detektion von Wasserstoff und n-Butanol bei verschiedenen Betriebstemperaturen; (ii) ZIF-8/CuO:Al-Hybridstrukturen für die Wasserstoff- und VOC-Sensorik unter widrigen Umweltbedingungen; (iii) Entwicklung von Multisensor-Arrays zur Differenzierung komplexer Analyten unter Verwendung von ZIFs/ZnO-Hybridstrukturen.

Wissenschaftliche Originalität und Neuheit der Forschung: Hybride Strukturen auf Basis von MOF-Metalloxid-Systemen, insbesondere ZIF/ZnO-Strukturen, wurden mittels eines einfachen und kostengünstigen Ansatzes entwickelt. Eine detaillierte Untersuchung der physikalisch-chemischen Eigenschaften der Hybridmaterialien auf ZIFs/ZnO- und ZIFs/CuO-Basis sowie die Etablierung einer Methodik zur Korrelation der Struktur-Eigenschaft-Leistungs-Beziehung für den selektiven Nachweis der getesteten Analyten – einschließlich VOCs und Wasserstoff unter widrigen Umweltbedingungen–stellt eine wissenschaftliche Neuerung dar, die für die Fachwelt von großem Interesse ist. Es wurde eine Methodik etabliert, die *In-situ*-Analysen mit sequenzieller Detektion zur umfassenden Gasdifferenzierung mittels mehrerer Sensoren kombiniert. Die Hybridstrukturen auf ZIF-8/CuO:Al-Basis zeigten eine beachtliche Sensitivität (75%) gegenüber 100 ppm Wasserstoff, selbst bei einer relativen Luftfeuchtigkeit von 81 %, was ihren Einsatz unter widrigen, feuchten Bedingungen über längere Zeiträume ermöglicht. Der entwickelte ZIF-71/CuO:Al-Hybridsensor wies eine duale Gasdetektion (n-Butanol und Wasserstoff) bei unterschiedlichen Betriebstemperaturen (200°C und 250°C) auf.

Die untersuchte wissenschaftliche Fragestellung: Die Forschungsarbeit etablierte Struktur-Eigenschaft-Leistungs-Korrelationen für Hybridstrukturen auf der Basis von metall-organischen Gerüstverbindungen (MOF) und Metalloxid-Systemen (MOF/MO), wie zum Beispiel ZIF-n (n = 67, 7, 71, 8) in Kombination mit Metalloxiden wie ZnO:Cd und CuO:Al. Dabei wurde der synergetische Effekt verschiedener Metalloxide in Kombination mit MOFs auf deren Gasdetektionsleistung gegenüber VOCs und Wasserstoff unter widrigen Bedingungen identifiziert. Die hochempfindliche und selektive Wasserstoffdetektion, selbst unter Bedingungen hoher Luftfeuchtigkeit und bei niedrigen Nachweisgrenzen, eröffnet neue Anwendungsbereiche.

Die theoretische Bedeutung und die Anwendungsgebiete der Arbeit: Die theoretische Bedeutung liegt in der Etablierung von Struktur-Eigenschaft-Leistungs-Beziehungen durch die Bestimmung der thermischen Stabilitätsbereiche und oxidativen Transformationspfade von metallorganischen ZIF-Gerüstverbindungen (ZIF-67, ZIF-7, ZIF-71 und ZIF-8) sowie Metalloxiden mittels *In-situ*-Strukturanalyse, wodurch deren fundamentale Betriebsgrenzen und mechanistische Beiträge zur Gassensorik definiert werden. Ebenso wurde ein kritisches Verständnis der radiolytischen Stabilität halogenierter MOFs durch die Identifizierung der röntgeninduzierten Degradation in ZIF-71 erarbeitet, wodurch aufgeklärt wurde, wie spezifische funktionelle Gruppen die strukturelle Integrität unter ionisierender Strahlung diktieren und welche Schwellenwerte für eine zerstörungsfreie Charakterisierung notwendig sind. Die Hybridstrukturen auf ZIF-8/CuO:Al-Basis zeigten eine selektive Detektion von Wasserstoff im Vergleich zu anderen getesteten Analyten, wobei eine niedrige Nachweisgrenze von ~402 ppb erreicht wurde, was für verschiedene Anwendungen, einschließlich der Detektion kleinster Wasserstoffleckagen, vorteilhaft ist. Hybridstrukturen auf ZIF-71/CuO:Al-Basis wiesen eine duale Gasdetektionsleistung für n-Butanol und Wasserstoff bei 200°C bzw. 250°C auf, wobei das Ansprechverhalten auf n-Butanol bei 200 °C viermal höher ist als auf Wasserstoffgas. Der ZIF-67/ZnO-Hybridsensor zeigte eine Ethanol-Selektivität bei 250°C, während bei den anderen drei Hybridstrukturen (ZIF-7/ZnO, ZIF-71/ZnO und ZIF-8/ZnO) eine Selektivität gegenüber Wasserstoff beobachtet wurde. Die praktischen Anwendungen der vorgestellten Arbeit liegen im Bereich der Wearable-Devices für die effektive Detektion von Wasserstoff und verschiedenen VOCs in Innen- und Außenbereichen und radiolytischer Detektion.

Umsetzung der wissenschaftlichen Ergebnisse: Die erzielten wissenschaftlichen Ergebnisse wurden teilweise am DMIB-FCIM der UTM implementiert; zudem wurde eine Patentanmeldung eingereicht.

RAJAT

POROUS NETWORKS OF NANOSTRUCTURED HYBRID MATERIALS

134.03 PHYSICS OF NANOSYSTEMS AND NANOTECHNOLOGIES

Summary of the doctoral thesis in physical sciences (UTM) and engineering (Kiel University)

Approved for printing:
Offset paper. RISO Typing
Print sheets 2.5

Paper size 60×84 1/16
Circulation 40 ex.
Order no.

UTM, MD 2004, mun. Chisinau, bd. Stefan cel Mare si Sfant, no. 168.
"TEHNICA-UTM" Publishing House
MD-2045, Chisinau mun., 9/9 Studentilor street